Payload-delivering engineered γδ T cells display enhanced cytotoxicity, persistence, and efficacy in preclinical models of osteosarcoma

Overline: CANCER

Authors: Fowler. D[1], Barisa. M[1], Southern. A[1], Nattress. C[2], Hawkins. E[1], Vassalou. E[1], Kanouta. A[1], Counsell. J, Rota. E[2], Vlckova. P[2], Draper. B[1], De Mooij[1], T., Farkas A.[1], Brezovjakova. H[1], Baker A. T.[1], Scotlandi. K[3], Manara. M. C[3], Tape. C[2], Chester. K[2], Anderson. J[1], Fisher. J[1*]

Affiliations:

1. UCL Great Ormond Street Institute of Child Health, Zayed Centre for Research, 20 Guilford Street, WC1N 1DZ, London, UK
2. UCL Cancer Institute, Paul O'Gorman Building, 72 Huntley Street, London, WC1E 6DD, UK
3. IRCCS Istituto Ortopedico Rizzoli, Experimental Oncology Laboratory, Via di Barbiano 1/10 40136 Bologna Italy

*Corresponding author. Email: jonathan.fisher@ucl.ac.uk

One Sentence Summary:

Opsonin-secreting γδ T cells exhibit potent antitumor activity against mouse models of osteosarcoma and represent an allogeneic cell therapy platform.

ABSTRACT

T cell-based cancer immunotherapy has typically relied on membrane-bound cytotoxicity enhancers such as chimeric antigen receptors expressed in autologous αβ T cells. These approaches are limited by tonic signaling of synthetic constructs and costs associated with manufacturing. γδ T cells are an emerging alternative for cellular therapy, possessing innate anti-tumor activity, potent antibody-dependent cellular cytotoxicity, and minimal alloreactivity. We present an immunotherapeutic platform technology built around the innate properties of the Vγ9Vδ2 T cell, harnessing specific characteristics of this cell type and offering an allo-compatible cellular therapy that recruits bystander immunity. We engineered γδ T cells to secrete synthetic tumor-targeting opsonins in the form of an scFv-Fc fusion protein and a mitogenic IL-15Rα–IL-15 fusion protein (stIL15). Using GD2 as a model antigen, we show that GD2-specific opsonin-secreting Vγ9Vδ2 T cells (stIL15-OPS-γδ T cells) have enhanced cytotoxicity and promote bystander activity of other lymphoid and myeloid cells. Secretion of stIL-15 abrogated the need for exogenous cytokine supplementation and further mediated activation of bystander natural killer cells. Compared to unmodified γδ T cells, stIL15-OPS-γδ T cells exhibited superior in vivo control of subcutaneous tumors and persistence in the blood. Moreover, stIL15-OPS-γδ T cells were efficacious against patient-derived osteosarcomas in animal models and in vitro, where efficacy could be boosted with the addition of zoledronic acid. Together the data identify stIL15-OPS-γδ T cells as a candidate allogeneic cell therapy platform combining direct cytolysis with bystander activation to promote tumor control.

Editor's Summary:

Both tumor antigen-specific antibodies and cellular therapies based on those antibodies, such as chimeric antigen receptor (CAR) T cells, have shown promise as cancer therapies. Here, Fowler *et al.* opted to combine the two and added a third feature – the use of γδ T cells instead of their αβ counterparts. The authors engineered γδ T cells, which have the potential to be used as an allogeneic therapy, to secrete opsonins that bound the tumor antigen GD2 and activated Fc receptors on immune cells. They also included an IL-15Rα-IL-15 fusion protein to further improve γδ T cell function and persistence. The opsonins produced by the γδ T cells activated the engineered cells as well as bystander immune cells in vitro and in vivo. This resulted in efficacy against multiple tumor models in vivo, including orthotopic patient-derived osteosarcomas, particularly when zoledronic acid was used as well. Together, these data support further development of opsonin-secreting γδ T cells as a cancer immunotherapy. –Courtney Malo

INTRODUCTION

Cellular immunotherapy using genetically modified T cells has shown striking success against hematological malignancies*(1)*. Synthetic immunotherapeutic modules such as chimeric antigen receptors (CARs), which link tumor-associated antigen recognition to T cell effector function, have been in development since the 1990s*(2).* There has, however, been a relative paucity of clinical success against solid tumors, driven in part by the highly immunosuppressive tumor microenvironment and poor penetration of the tumor by the engineered cells.

Vγ9Vδ2 T cells are a versatile subset for cellular immunotherapy, possessing many helpful properties that include potent antibody-dependent cellular cytotoxicity (ADCC) capacity*(3–6),* a tissue-tropic homing profile*(7)*, and a range of innate tumor-sensing receptors minimizing the likelihood of tumor escape*(8)*. Furthermore, γδ T cells are straightforward to expand to clinically useful numbers*(6, 9, 10)*, cause minimal graft-versus-host disease in the allogeneic setting*(11)* and, when present in the tumor microenvironment, are a strong positive correlate with good clinical outcome*(12, 13)*. This combination of features makes Vγ9Vδ2 T cells an attractive candidate for engineered cell therapy.

Although progress has been made in “armoring” CAR-T with secreted cytokines, most T cell engineering strategies rely on membrane-bound constructs. This confines any enhanced activity to the engineered cells; un-engineered cells in the product and bystander immune cells receive little, if any, benefit. We sought to overcome these challenges by designing an allo-compatible cell therapy platform producing secreted mediators only: a synthetic tumor-targeting antibody-like opsonin in the form of an scFv-Fc fusion protein (SFP), and a mitogenic interleukin 15 receptor (IL-15R)α-IL-15 cytokine

fusion protein referred to as stIL15. Containing the variable portions of both the heavy and light chains of an antibody, fused to the constant region of the heavy chain, scFv-Fc fusion proteins have a smaller genetic footprint than whole antibodies and form homodimers in solution. We demonstrated that the combination of engineered cytokine armoring and opsonin production drives Vγ9Vδ2 T cell product persistence and activity, as well as direct and bystander cytotoxicity in a manner that can be enhanced with zoledronic acid (ZOL) combination treatment. Moreover, we evaluated the therapeutic efficacy of these engineered γδ T cells using patient-derived preclinical models of osteosarcoma.

RESULTS

γδ T cells can be engineered to deliver multiple immune-active secreted payloads

The nomenclature used to describe the various cell types in this manuscript is outlined in table S1. To indicate the binder specificity of cells that have been engineered to express constructs encoding antigen-targeting SFP or CAR, the nomenclature is prefixed with the antibody clone from which the scFv component was derived, as listed in table S2; for example, γδ T cells engineered to secrete GD2-specific SFP are referred to as “14G2a OPS-γδ T cells”.

Vγ9Vδ2 cells from healthy donors were expanded and transduced with viral vectors to constitutively express either a secreted SFP, a secreted IL-15 construct, or both (fig. S1A and S1B), preceded by either a CD34 tag or GFP marker gene. Genes encoding proteins were separated by virally-derived 2A sequences, which induce ribosomal skipping with subsequent separated protein product translation. Transduction efficiencies and Vγ9Vδ2 purities of each preparation are shown in fig. S1C. We show that cells can be transduced to secrete SFP against a range of tumor-associated antigens, including GD2, CEACAM5, and CD20 (binder-specific scFv sequences are listed in the Supplementary Materials and Methods). Binder production was validated by incubating target cells with respectively-transduced cell supernatant, followed by detecting opsonization through staining the labelled target cells with a secondary anti-Fc monoclonal antibody (mAb) (Fig. 1A and fig. S1D). We chose to focus on GD2-targetting binder 14G2a as a model to evaluate OPS-γδ T cell functional performance. GD2 is a proven immunotherapeutic target expressed on neuroblastoma, Ewing sarcoma, and osteosarcoma*(14–17)*, with limited expression in healthy tissue.

Figure 1

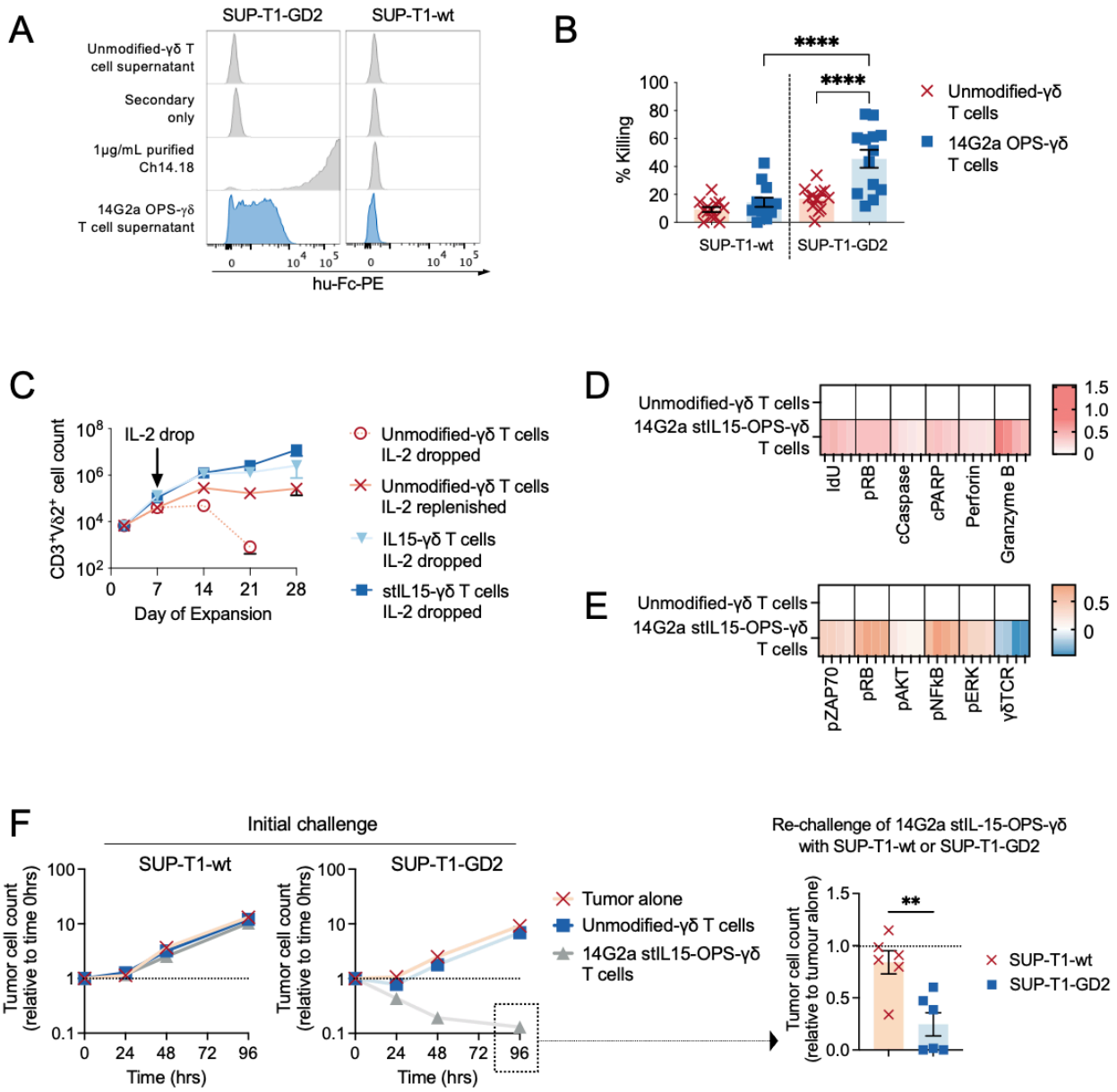

Figure 1: γδ T cells can be engineered to deliver multiple immune-active secreted payloads. **(A)** Flow cytometry of SUP-T1-wt and SUP-T1-GD2 cells exposed to culture supernatant from either unmodified-γδ T cells or 14G2a OPS-γδ T cells. Phycoerythrin (PE)-conjugated anti-human Fc was used to detect SFP binding. 1μg/mL purified whole IgG1 against GD2 (Ch14.18) was used as a positive control. Representative plots from 3 donors are shown. **(B)** Percentage killing as measured by flow cytometry of SUP-T1-wt and SUP-T1-GD2 cells by unmodified-γδ T cells or 14G2a OPS-γδ (n = 13 across 13 donors) in an overnight co-culture at an E:T ratio of 1:1. Statistical comparisons are from one-way ANOVA with Sidak's multiple comparison correction. **(C)** $CD3^+V\delta2^+$ T cell counts over time during the expansion of unmodified-γδ T cells, IL15-γδ and stIL15-γδ as measured by flow cytometry. Cultures were supplemented with IL-2 every 2-3 days either continuously ("IL-2 replenished") or only up until day 7 ("IL-2 dropped"). Data from n=3 to 6 donors. **(D and E)** Expression of key markers of cell signaling, cell cycle, apoptosis,

and cytotoxic function (D) as well as phosphorylation of TCR signaling mediators (E) were assessed in unmodified-γδ or 14G2a stIL-15-OPS-γδ T cells on day 12 of expansion using mass cytometry. Differences were normalized to unmodified-γδ T cells as the baseline and heatmaps show EMD of n=4 across 2 donors (2 replicates per donor). **(F)** SUP-T1-wt and SUP-T1-GD2 cell counts over time as measured by flow cytometry during initial challenge at an E:T of 1:1 and then following post-clearance re-challenge. n=3 for tumor alone, n=6 across 2 donors for co-cultures. Statistical comparison is from an unpaired t test. **p<0.01, ****p<0.0001. Data are presented as mean ± SEM.

The restriction of GD2 expression to specific tissues facilitates use of isogenic $GD2^+$ and $GD2^-$ lines to determine antigen-specific effects. Cytotoxicity of unmodified-γδ T cells against wild-type SUP-T1 (SUP-T1-wt, a T cell lymphoblastic lymphoma cell line), which do not express GD2, and SUP-T1-GD2, engineered to express high amounts of GD2, was equivalent (fig. S1E). Supernatant from 14G2a OPS-γδ T cells contained 6.1±1.7ng/ml anti-GD2 SFP at day 12 of expansion (n=3 representative donors, determined by flow cytometry standard curve method), equivalent to 3.97±1ng per $1x10^6$ cells (fig. S1F). In GD2 isogenic SUP-T1 models, 14G2a OPS-γδ T cells displayed enhanced antigen-specific cytotoxicity compared to unmodified-γδ T cells (Fig. 1B). Although 14G2a OPS-γδ T cells had lower cytotoxicity than 2^{nd} generation 14G2a 28ζ CAR-γδ T cells in short-term killing assays (fig. S2A and B), in longer-term (7 day) co-cultures their ability to control SUP-T1-GD2 growth was equivalent to that of the CAR-γδ T cells, consistent with the requirement for opsonin accumulation to effect OPS-γδ T cell cytotoxicity (fig. S2C). We then compared the checkpoint receptor phenotype of OPS- and CAR-γδ T cells in the absence of target exposure. 14G2a OPS-γδ T cells and CAR-

γδ T cells were harvested from manufacture at day 10 and analyzed by flow cytometry. Compared to CAR-γδ T cells, OPS-γδ T cells showed significantly lower expression of checkpoint receptors TIM-3, LAG-3, and TIGIT (*p <0.0001 in all cases by one way ANOVA*), consistent with target-independent signaling mediated by CAR- but not OPS-constructs (fig. S2D).

IL-15 is a proliferation-supporting cytokine commonly used in γδ T cell expansion protocols*(6, 10, 18, 19)*. γδ T cell dependence on its exogenous supply has been previously described *(20)*. Armoring of γδ T cells with membrane bound IL-15 is clinically beneficial *(21)*. The activity of IL-15 can be enhanced by generating a fusion protein with the sushi domain of IL-15Rα*(22, 23)*; we denote this 'stabilized IL-15' or 'stIL15'. Such stabilized IL-15 constructs have been used both as drugs in their own right and as armoring strategies for CAR-αβ T cells*(23–27)*. We genetically modified γδ T cells to secrete either IL-15 or stIL15, using eGFP as a marker of transduction. Transduction efficiencies were higher for the eGFP-2A-stIL15 construct compared to eGFP-2A-IL-15, despite equal multiplicity of infection (MOI) of lentiviral vector used (fig. S3A and B).

To investigate the dependence of expanding unmodified or cytokine-engineered γδ T cells on exogenous cytokine support for sustained expansion, we compared γδ T cell expansion over 14 to 28 days in cultures that were either continuously supplemented with 100U/ml IL-2 or supplemented up to day 7 only (fig. S3C). γδ T cells engineered to secrete IL-15 or stIL15 continued to expand in the absence of exogenous IL-2 support, but unmodified-γδ T cell numbers collapsed once IL-2 was removed, consistent with a requirement of external cytokine support for unmodified-γδ T cell maintenance (Fig. 1C). γδ T cells engineered with the eGFP-2A-stIL15 cassette yielded higher concentrations of detectable cytokine than native IL-15, irrespective of IL-2 supplementation (fig. S3D). Due

to the higher transduction efficiency and amount of detectable secreted protein observed with stIL15-γδ T cells compared to IL-15-γδ T cells, we progressed the stIL15 module for further testing.

We interrogated the effects of stIL15 on γδ T cell signaling using mass cytometry followed by Earth Mover's Distance (EMD) analysis to determine differences in abundance of key signaling and phenotypic *(28)*. Compared to unmodified-γδ T cells, stIL15-γδ T cells had increased abundance of phosphorylated (p) signal transducer and activator of transcription 5 (STAT5), protein kinase B (AKT), extracellular signal-regulated kinase (ERK) and nuclear factor kappa-light-chain enhancer of activated B cells (NFκB (p65/RelA)), consistent with IL-15-driven responses (fig. S3E). stIL15-γδ T cells showed higher markers of proliferation (iododeoxyuridine (IdU) incorporation and phosphorylated retinoblastoma protein (Rb)) without concurrent upregulation of apoptotic markers such as cleaved poly(ADP-ribose) polymerase (PARP) or cleaved Caspase 3, suggesting that stIL15-γδ T cells are more activated but no more prone to apoptosis than donor-matched unmodified-γδ T cells (fig. S3E). Consistent with a more favorable tumor-targeting profile, stIL15-γδ expressed higher CD16, CD95L (FAS-L), TNF-related apoptosis-inducing ligand (TRAIL), DNAX accessory molecule 1 (DNAM1) and NKp30, though NKp44 expression was not affected (fig. S3F). In the absence of any additional cytokine support, stIL15-γδ T cells were still detectable in the blood of immunodeficient mice challenged with an intratibial injection of a $GD2^{+}$ osteosarcoma line 14 days after intravenous infusion, whereas unmodified-γδ T cells and 14G2a 28ζ CAR-αβ T cells were not, indicating that stIL15 armoring enhanced γδ T cell persistence in the absence of exogenous human cytokine supplementation (fig. S4A).

Having separately demonstrated the benefit of the OPS- and stIL15-modules, we combined them to produce stIL15-OPS-γδ T cells (fig. S1B). Transduction efficiency using RDPro-pseudotyped lentivector remained high (75±2.5% mean±SEM for n=13 over 8 representative donors) and co-expression of stIL15 and SFP opsonin was demonstrated by enzyme-linked immunosorbent assay (ELISA) and flow cytometry, respectively (fig. S4B and C). When 14G2a stIL15-OPS-γδ T cells were harvested at day 12 of expansion and re-seeded into fresh media, opsonin yield 72 hours later was higher than that observed from OPS-γδ T cells at matched T cell density (fig. S4D), with a yield of 1.55±0.05ng per 10^6 cells seeded (mean of n=3 representative donors). Western blot analysis confirmed the presence of secreted, dimerized opsonin in 14G2a stIL15-OPS-γδ T cell supernatant (107.4kDa), with no detection of monomeric opsonin (53.7kDa, fig. S4E). Although OPS-γδ T cells produced opsonins, the production appeared to falter over time, whereas stIL15-OPS-γδ T cells displayed sustained opsonin secretion. This is possibly due to the more favorable expansion kinetics and activation profile conferred onto γδ T cells by stIL15 engineering. Indeed, 14G2a stIL15-OPS-γδ T cells showed enhanced expansion and Vγ9Vδ2 cell purity compared to unmodified-γδ T cells (fig. S4F and G). Provided appropriate and regular media replenishment and cell splitting, cytokine armoring enabled 14G2a stIL15-OPS-γδ T cells to continue expanding for a month following transduction (fig. S4H).

Compared to unmodified-γδ T cells, stIL15-OPS-γδ T cells retained the increased IdU incorporation and pRB observed in stIL15-γδ T cells but also had increased expression of apoptosis-associated cleaved caspase 3 and cleaved PARP (Fig. 1D, fig. S5A). Consistent with their enhanced activation and cytotoxicity, stIL15-OPS-γδ T cells had higher expression of Perforin and Granzyme B compared with unmodified-γδ T cells (Fig. 1D and fig. S5B). Indicative of activation-related transcriptional changes, 14G2a

stIL15-OPS-γδ T cells had elevated pNFκB abundance, also showing evidence of intracellular signaling typical of T cell activation, including ITAM-dependent phosphorylated zeta-chain associated protein kinase 70 (pZAP70), as well as pAKT and pERK with relative downregulation of the γδ T cell receptor (TCR) (Fig. 1E and fig. S5C).

Cytotoxicity of 14G2a stIL15-OPS-γδ T cells was antigen-specific when measured against isogenic SUP-T1-wt ($GD2^-$) or SUP-T1-GD2 ($GD2^+$) targets; moreover, cytotoxicity was persistent in an in vitro re-challenge system (Fig. 1F, fig. S5D). 14G2a stIL15-OPS-γδ T cells but not unmodified-γδ T cells continued to proliferate following the initial tumor challenge, though proliferation in response to the antigen positive SUP-T1-GD2 cells was attenuated compared with the antigen negative SUP-T1-wt (fig. S5E). Furthermore, 14G2a stIL15-OPS-γδ T cells showed continued proliferation following re-challenge (fig. S5E). Overall, this suggests that serial killing by γδ T cells carries a proliferative cost that can be partially but not fully rescued by γδ T cell armoring with cytokine. In addition to the isogenic SUP-T1 model, we also tested cytotoxicity against the Kelly neuroblastoma cell line, which endogenously expresses GD2 (fig. S5F). Compared with unmodified-γδ T cell and stIL15-γδ T cell controls, 14G2a stIL15-OPS-γδ T cells displayed enhanced cytotoxicity against this cell line (fig. S5G).

To evaluate 14G2a stIL15-OPS-γδ T cell efficacy in vivo, NOD.Cg-*Prkdc*^{scid} *Il2rg*^{tm1Wjl}/SzJ (NSG) mice bearing subcutaneous SUP-T1-GD2 tumors received a single intravenous dose of $1x10^7$ unmodified-γδ T cells or 14G2a stIL15-OPS-γδ T cells without further cytokine support (Fig. 2A, and fig. S6A). Zoledronic acid treatment was not employed in this in vivo model. Tumor progression was monitored using bioluminescence and caliper measurements. To evaluate T cell persistence, blood samples were collected on day 7 post-T cell administration. Mice treated with 14G2a

stIL15-OPS-γδ T cells had higher circulating $CD3^{+}V\delta2^{+}$ cell numbers in their blood than mice treated with unmodified-γδ T cells (Fig. 2B). Tumor luminescence and size comparisons were censored 10 days after treatment (15 days after engraftment) when the first animals met the experimental endpoint of tumors >10mm in any dimension. At this point, tumor luminescence and volume were lower in animals treated with stIL15-OPS-γδ T cells compared with unmodified-γδ T cells (Fig. 2C and fig. S6B to D). γδ T cell engineering with the 14G2a stIL15-OPS construct enhanced animal survival, whereas unmodified-γδ T cells conferred no survival benefit (Fig. 2D). Together, these data demonstrate the efficacy of stIL15-OPS-γδ T cell therapy.

Figure 2

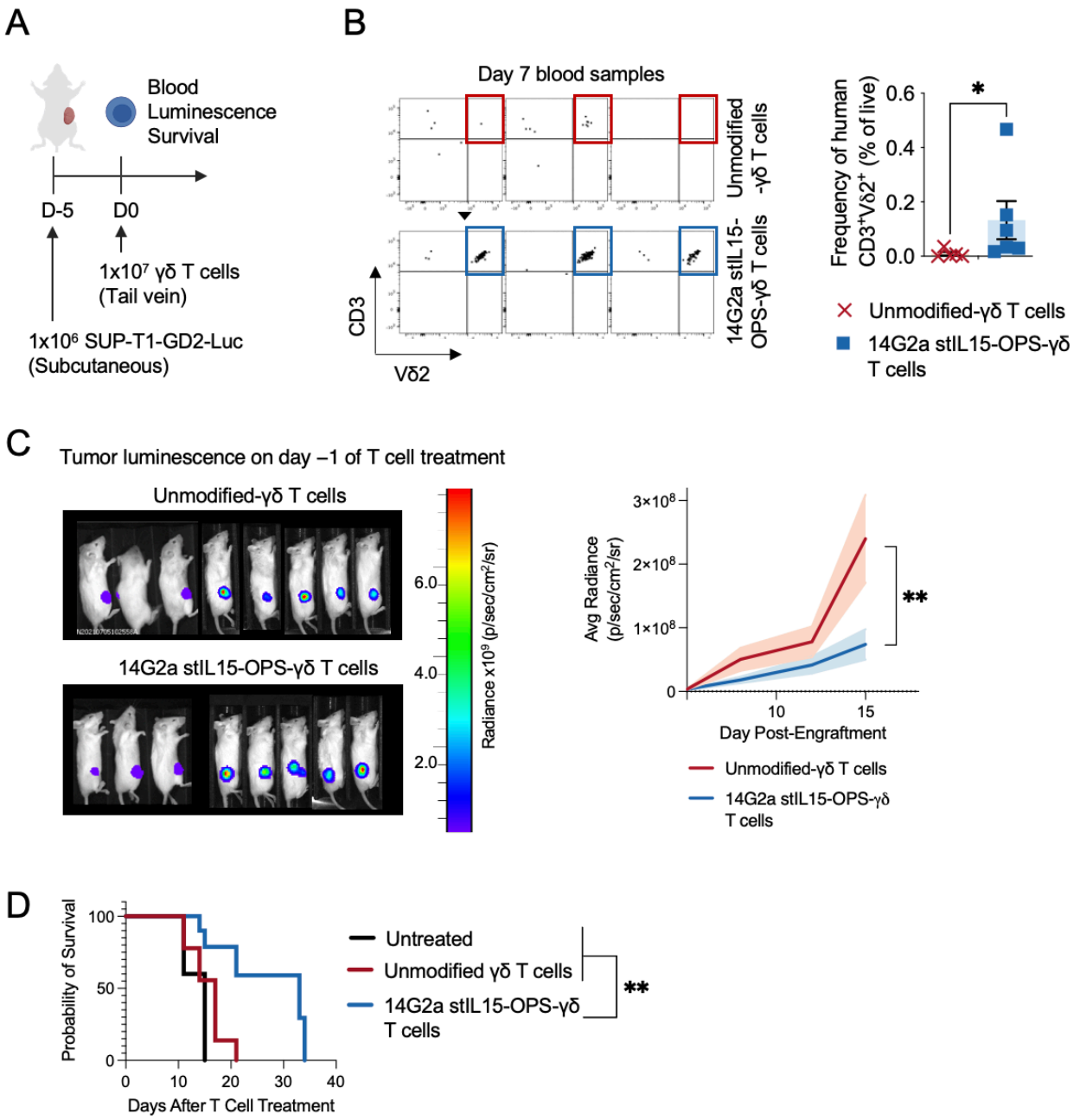

Figure 2: stIL15-OPS-γδ cells are efficacious against antigen-positive tumor targets in vivo. (A) NSG mice were challenged with a subcutaneous (Subcut) injection of $1x10^6$ luciferase-expressing SUP-T1-GD2 cells (SUP-T1-GD2-Luc) in Matrigel. Five days later, mice were treated with a tail vein injection of either $1x10^7$ unmodified-γδ (n= 8) or 14G2a stIL15-OPS-γδ (n= 8) or left untreated (n= 5). Data is pooled from two independent experiments: a pilot study and a follow-up study. Blood samples were taken to track cell survival, and serial bioluminescence measurements were used to track tumor growth and efficacy over time. **(B)** Flow cytometry was used to detect human $CD3^+V\delta2^+$ γδ T cells in day 7 blood samples. Representative plots from 3 mice per group showing CD3 and Vδ2

expression within the viable human CD45$^+$ population. Shown are individual data points (left) and means±SEM (right) for the frequency of CD3$^+$Vδ2$^+$ γδ T cells within gated live cells from all mice. Statistical comparison is from a Mann-Whitney test. **(C)** *Left:* Bioluminescence images of treatment groups at day -1 of T cell treatment. *Right:* Bioluminescence plotted as average radiance over time. Data are presented as means±SEM with area fill within error bands; statistical comparisons were determined used mixed-effects analysis and the p-value shown is for the interaction of time and treatment. **(D)** When tumors exceeded 1cm by vernier caliper measurement in any one direction, mice were euthanized, and these data were used to calculate survival curves. Statistical comparison is from a Mantel-Cox survival curve comparison test. *p<0.05, **p<0.01.

Engineered γδ T cells improve the entire cell therapy product, not only the portion that expresses the transgene

In contrast to immunotherapies such as CAR-T cells that use membrane-bound enhancers of cellular activity, stIL15-OPS-γδ T cell-secreted payloads have the potential to influence both transduced cells and non-transduced bystanders. Evaluation of the differential effects of membrane-bound and secreted constructs on T cell signaling requires a means of accurately determining the dependence of signaling markers on the presence of transgenes at a single-cell level. As representative and relevant membrane-bound immunotherapeutic comparators, we generated CAR-αβ T cells using three different 2nd generation CAR constructs, targeting either GD2, CD33, or ALK, with CH2CH3 spacers, CD28 transmembranes and CD28-CD3ζ endodomains (fig. S7A).

For CAR-αβ T cells, we analyzed the differences in marker abundance by comparing CAR$^+$ and CAR$^-$ cells in the same sample, whereas stIL15-OPS-γδ T cells were compared to donor and time-matched unmodified-γδ T cells to eliminate the

confounding effect of the secreted product. Simple correlative measure can over-emphasize the influence of denser areas of a distribution, neglecting biologically informative outliers. We therefore used Density Rescaled Visualization (DREVI) plots and Density Rescaled Estimates of Mutual Information (DREMI) scores*(29)* to illustrate the relationship between transgene expression and signaling markers. DREMI describes the strength of relationship or "edge strength" between two markers. A brief overview of DREVI and DREMI derivation is shown in Fig. 3A, and the sample handling for these comparisons is shown in fig. S7B. A high DREMI score for a given edge X-M indicates that M is highly dependent on X, whereas a low DREMI score indicates that they are independent of each other. The magnitude of the DREMI score indicates the degree of codependence, and the plasticity of DREMI scores indicates the ability of this relationship to change depending on the stimulus provided.

DREVI was used to visualize the relationship between pERK and transgene expression; GFP was used as a marker of stIL15-OPS expression whereas membrane-bound CARs were directly stained for the Fc stalk. CAR-pERK DREVI plots indicated a clear increase in pERK as CAR expression increased, whereas stIL15-OPS-γδ T cells had steady pERK abundance throughout all cells in the product regardless of GFP expression (Fig. 3B). These differences were reflected in the DREMI scores. CAR-pERK DREMI scores were high, whereas GFP-pERK scores were low (Fig. 3C). Similar DREVI profiles were observed for the 14G2a stIL15-OPS-γδ T cell GFP-pZAP70, GFP-pAKT and GFP-pNFκB edges, suggesting a lack of direct association between γδ T cell product transduction efficiency and signaling (Fig. 3D). Focusing on species known to be influenced by 28ζ CAR signaling, we observed high DREMI scores for the CAR-pERK, CAR-pNFκB and CAR-TIM-3 edges for CAR-αβ products analyzed; the effect was

particularly pronounced for the CAR-pERK and CAR-TIM-3 edges, even in the absence of exposure to CAR cross-linking (Fig. 3E). In contrast, despite evidence that stIL15-OPS-γδ T cell engineering increases abundance of many signaling species (as shown in Fig. 1E), the strength of relationship between these markers and GFP expression remained low (Fig. 3F).

Taken together, the “effect of transduction”, which can be derived from the change in marker abundance (EMD) between transduced and unmodified-γδ T cells, and the “dependence on transgene” which can be derived from the DREMI score for edges

beginning with the transduction marker (CAR-A, B, C or GFP-A, B, C) give an overall

Figure 3

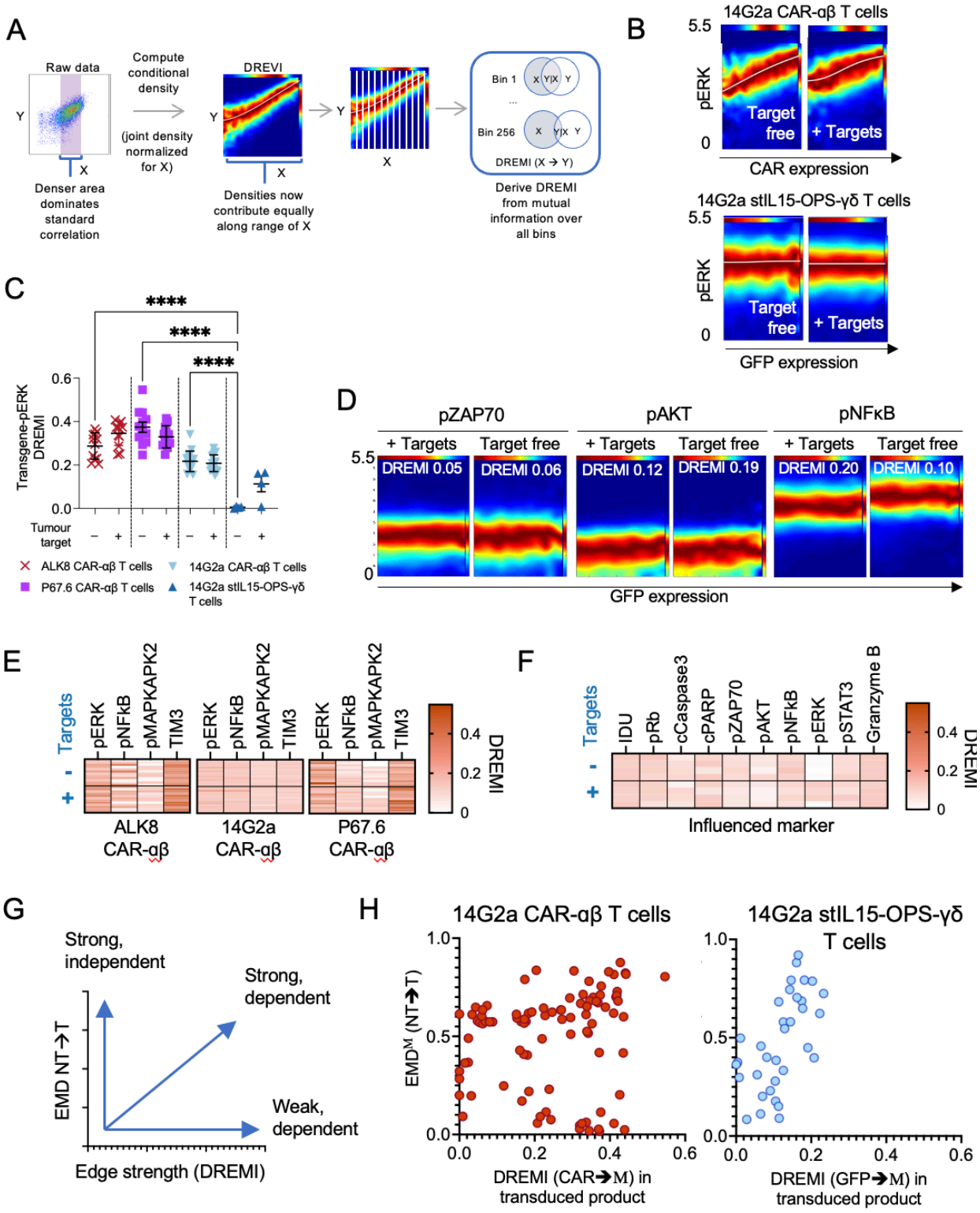

Figure 3: Secreted products avoid dependence on transgene expression for enhancement of antitumor immunity. (A) Example DREVI/DREMI analysis of correlation between molecules X and Y. A high DREMI score with a steep gradient on

DREVI indicates that Y expression is highly dependent on X. **(B)** Comparison of X-pERK DREVI plots and DREMI scores for representative 14G2a CAR-αβ T cells (n= 3 across 3 donors) and 14G2a stIL15-OPS-γδ T cells (n=4 across 2 donors) in the presence or absence of GD2+ targets (Sup-T1 GD2), where X is the marker of transduction. The first component of the DREMI score and X-axis of the DREVI plots is either directly stained CAR expression, or GFP in the case of stIL15-OPS-γδ T cells, which lack a membrane-bound marker. For C to F, the antigen expressing target cells are as follows: ALK: Sup-T1-ALK, GD2: SUP-T1 GD2, CD33: MV4-11. **(C)** DREMI scores for the interaction between the transgene and pERK in ALK8 CAR-αβ |(targeting ALK), 14G2a CAR-αβ (targeting GD2), P67.6 CAR-αβ (targeting CD33), and 14G2a stIL15-OPS-γδ T cells in the presence or absence of antigen-positive targets. Each point represents a single donor and stimulation condition. Statistical comparisons are from one-way ANOVA with Sidak's multiple comparison correction. ****p<0.0001. Data are presented as mean±SEM **(D)** DREVI plots showing the lack of association between transduction (as shown by GFP expression) and abundance of pZAP70, pAKT, or pNFκB in 14G2a stIL15-OPS-γδ T cells in the presence or absence of antigen-positive targets. **(E and F)** DREMI scores describing the influence of transgene expression on markers known to change expression in response to transgene activity in ALK8, 14G2a and P67.6 CAR-αβ T cells (E) and 14G2a stIL15-OPS-γδ T cells (F). **(G)** Across all markers measured by mass cytometry, plotting the size of the effect (as measured by EMD between non-transduced (NT) and transduced (T)) in the entire population against the dependence of the effect on transgene expression (as measured by DREMI) gives information on strength and transgene dependence. **(H)** Transduction-dependent, product-wide effect size plotted against dependence on trans-gene expression at a single-cell level for 14G2a CAR-αβ T cells and 14G2a stIL15-OPS-γδ T cells.

picture of signaling behavior these two engineered product types. Markers with high transduction-induced EMD and high DREMI scores indicate strong signals only in cells expressing the transgene, whereas high transduction-induced EMD but low DREMI scores indicate strong signals independent of the transgene (Fig. 3G). Signals in unstimulated 14G2a CAR-αβ and 14G2a stIL15-OPS-γδ T cell products were analyzed. The transduction-induced EMD for a given marker (M) was plotted against that marker's dependence on the transgene (DREMI transgene-M), using all markers where an effect of transduction had been identified. The CAR-αβ plot was enriched in the "strong, dependent" area, indicating that the tonic signaling observed in the CAR-αβ population

was highly dependent on the presence of the detectable CAR molecules in the cell. Conversely, whilst there were strong signals detected in 14G2a stIL15-OPS-γδ T cells, the plots were enriched in the “strong, independent” region, demonstrating that the detected changes did not require the transgene to be present in an individual cell for that cell to benefit (Fig. 3H).

Having demonstrated that 14G2a stIL15-OPS-γδ T cell engineering confers benefits to both transduced and non-transduced cells within the product, we investigated if these benefits could be conferred to other bystander immune cells (fig. S8A). We evaluated the ability of 14G2a OPS-γδ and stIL15-OPS-γδ T cell supernatant to engage the antigen-specific cytotoxicity of ADCC/ADCP-competent cells such as unmodified-γδ T cells (Fig. 4A), NK cells (Fig. 4B) and macrophages (Fig. 4C). Supernatant from 14G2a

Figure 4

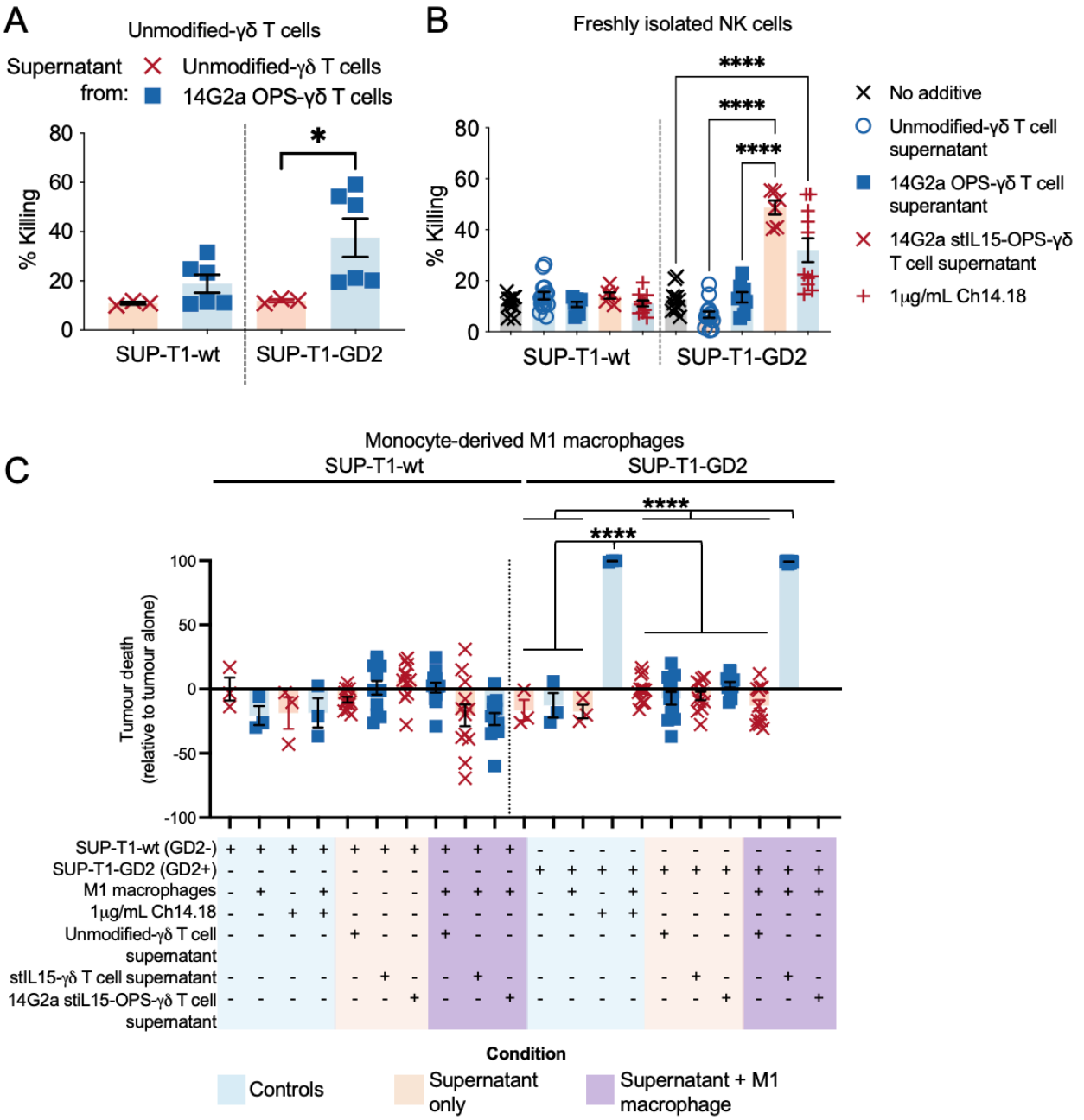

Figure 4: stIL15-OPS-γδ recruit bystander cells to elicit ADCC and ADCP responses against antigen-positive tumor target cells. Flow cytometry was used to measure the effect of supernatant from unmodified-γδ, 14G2a OPS-γδ or 14G2a stIL15-OPS-γδ T cells on percentage killing of SUP-T1-wt and SUP-T1-GD2 cells co-cultured overnight with unmodified-γδ T cells (**A**, n = 3 to 6 across 2 supernatant and 2 T cell donors), NK cells isolated from the peripheral blood of healthy donors (**B**, n=6 to 15 using 4 NK cell donors and 4 γδ T cell supernatant donors), and monocyte-derived M1 macrophages (**C**, n=12 supernatants from 4 donors and macrophages generated from one donor). Individual data

points and means ± SEM are shown. For **(A)** and **(B)** the E:T ratio is 1:1, for **(C)** target cells were added to a monolayer of monocyte-derived macrophages. 1μg/mL purified whole Ch14.18 was used as a positive control. For statistical comparisons, one-way ANOVA with Sidak's **(A and B)** or Tukey's **(C)** multiple comparisons corrections were used. *p<0.05, ****p<0.0001.

OPS-γδ T cells (without stIL15) induced antigen-specific cytotoxicity in bystander cells (assay setup and bystander cell differentiation illustrated in fig. S8B) such as unmodified-γδ T cells (Fig. 4A), and neutrophils (fig. S8C), but did not enhance NK cell cytotoxicity despite their demonstrable ADCC activity mediated by the addition of 1 μg/mL of Ch14.18 (Dinutuximab beta) mAb (Fig. 4B). IL-15 has been described as a potent stimulator of NK cell effector function and differentiation*(30)*; unlike OPS-γδ T cell supernatant, stIL15-OPS-γδ T cell supernatant mediated substantial antigen-specific NK cell cytotoxic enhancement (Fig. 4B), indicating that NK cell cytotoxicity requires additional stimulation that can be conferred by an IL-15-like signal. Supernatant from 14G2a stIL15-OPS-γδ T cells, but not stIL15-γδ T cells, mediated efficient macrophage clearance of GD2-positive tumor cells, whereas GD2-negative targets were spared, underscoring the requirement of both opsonin and target antigen for OPS-γδ T cells secreted transgenes to engage macrophage ADCP (Fig. 4C).

Analysis of FcγR and chemokine receptor expression in engineered γδ T cells

After initial expansion with zoledronic acid and IL-2 but before transduction, Vγ9Vδ2 γδ T cells expressed high amounts of CD16b and CD64, with moderate CD32 expression. CD16a was only present on a very small subset of cells (Fig. 5A). Following

engineering to form 14G2a OPS-γδ T cells, CD16b expression was lost but there was a marked but variable increase in CD16a expression, such that this isoform comprised the entirety of CD16 expression at γδ T cell harvest at day 10 of culture. CD32 and CD64 expression did not change (Fig. 5A).

Because cytotoxicity of 14G2a OPS-γδ T cells against antigen-positive SUP-T1-GD2 targets varied (Fig. 1D) and CD16a expression showed donor-to-donor variability whereas CD32 and CD64 expression were consistent, we hypothesized that variations in the interplay between low opsonin concentration and CD16 expression may govern Vγ9Vδ2 ADCC and thus OPS-γδ T cell cytotoxicity. γδ T cells with higher CD16 expression (as detected by a pan-CD16 antibody recognizing both CD16a and CD16b) were more cytotoxic at opsonin concentrations in the 1 to 10ng/mL range (Fig. 5B). At 1.6 ng/mL of Ch14.18 anti-GD2 antibody, the percentage of CD16 expression required to achieve 50% target killing was 58.1% (95% CI 44.9 to 76.6%) with strong correlation between cytotoxicity and CD16 expression (Pearson $R^2 = 0.77$, $p<0.0001$, Fig. 5C, FcγRIII gating shown in fig. S9A). This correlation was lost at high (1μg/mL) Ch14.18 mAb

Figure 5

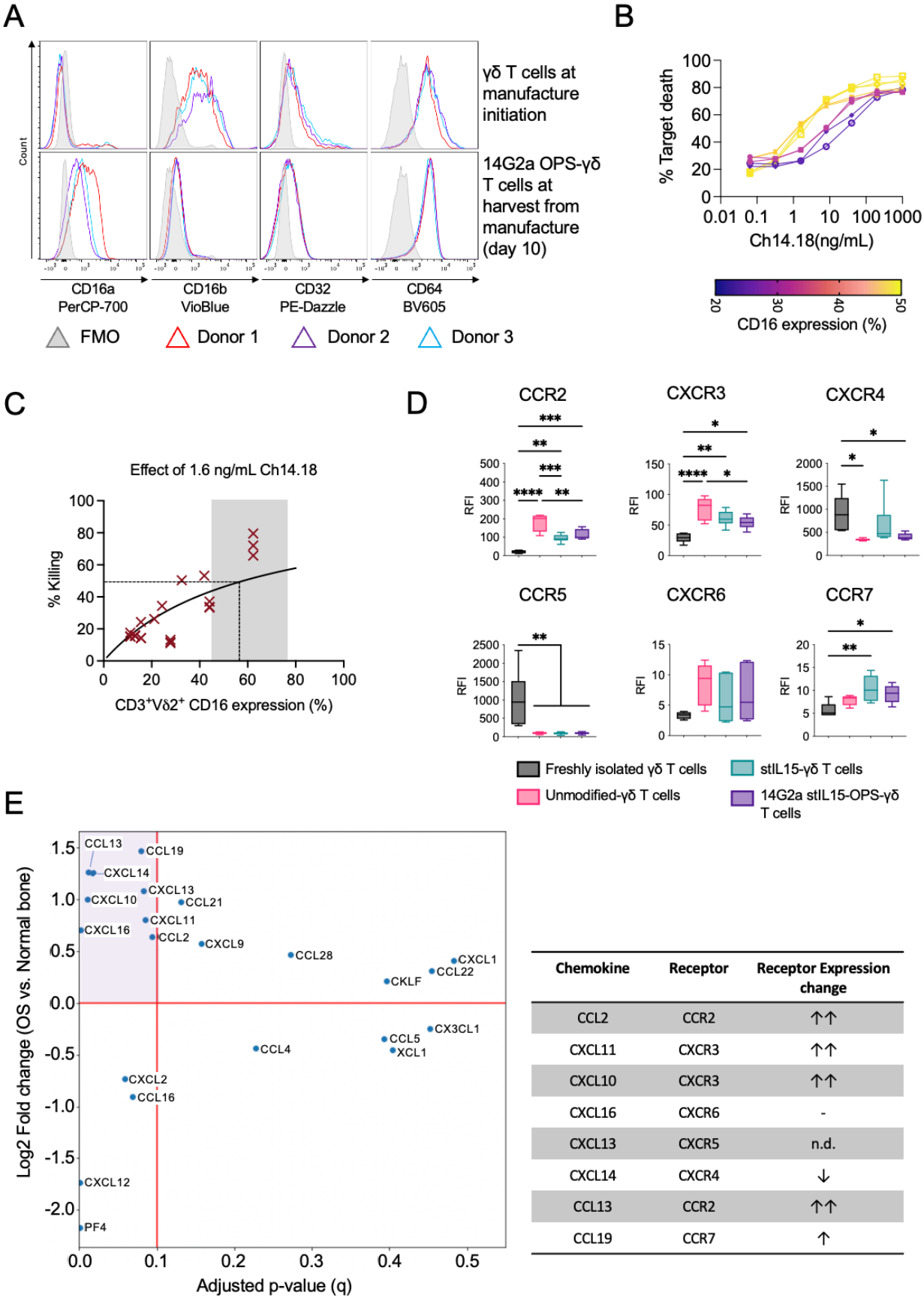

Chemokine	Receptor	Receptor Expression change
CCL2	CCR2	↑↑
CXCL11	CXCR3	↑↑
CXCL10	CXCR3	↑↑
CXCL16	CXCR6	-
CXCL13	CXCR5	n.d.
CXCL14	CXCR4	↓
CCL13	CCR2	↑↑
CCL19	CCR7	↑

436

Figure 5: stIL15-OPS-γδ T cell phenotype favors ADCC and osteosarcoma-homing. **(A)** Expression of CD16a, CD16b, CD32 and CD64 on Vδ2$^+$ γδ T cells was measured by flow cytometry after stimulation with 5μM zoledronic acid plus IL-2, before and 10 days after transduction to form 14G2a OPS-γδ T cells. FMO, fluorescence minus one control. **(B)** Killing of SUP-T1-GD2 by unmodified-γδ T cells in the presence of varying concentrations of Ch14.18 antibody (5-fold serial dilution ranging from 0.064ng/mL to 1μg/mL). n=9 across 4 donors. Donor lines are colored by the percentage expression of CD16 on CD3$^+$Vδ2$^+$ cells post expansion. **(C)** Killing of SUP-T1-GD2 by unmodified-γδ T cells in the presence of 1.6ng/ml Ch14.18, plotted against expression of CD16 on the corresponding donor's Vδ2 T cells after expansion. Least squares curve fitting was used to determine the half-maximal effective concentration (EC_{50}) for CD16 expression, n=22 across 10 donors. Dotted line indicates the EC_{50} and the gray shaded area represents the 95% confidence interval. For **(B)** and **(C)**, CD16 expression was assessed using a pan-CD16 antibody that recognizes both CD16a and CD16b. **(D)** CCR2, CXCR3, CXCR4, CCR5, CXCR6 and CCR7 expression on gated Vδ2$^+$ cells within freshly isolated PBMCs was compared with unmodified-γδ, stIL15-γδ or 14G2a stIL15-OPS-γδ T cells on day 12 of expansion as assessed by flow cytometry. Relative fluorescence intensity (RFI) values for each marker are shown. Box and whisker plots show mean and 5 to 95th centile for n=6 donors. Statistical comparisons are one-way ANOVA with Tukey's multiple comparison correction, *p<0.05, **p<0.01, ***p<0.001, ****p<0.0001. **(E)** Differential expression of chemokines in osteosarcoma compared to normal bone from the same patient (n=18); table indicates the receptor expression changes from **(D)** in the context of osteosarcoma chemokine enrichment. n.d. = not done.

concentration, where the percentage CD16 expression needed to mediate 50% killing at 1:1 E:T ratio was 6.4% (95% CI 4.5 to 8.8%), to the extent that the curve rapidly plateaued with poor correlation (Pearson R^2 = 0.2, p = 0.0094, fig. S9B). Transduction with GFP-IL15, GFP-stIL15 or GFP-stIL15-14G2a constructs had minimal effect on CD16 expression compared to unmodified-γδ T cells (fig. S9C). CD16 expression is therefore a potentially useful biomarker for selecting optimal allogeneic cell therapy donors for OPS-γδ T cell product manufacturing*(31)*, and subsequent cytotoxicity data is presented on CD16^{hi} (>40% expression) Vγ9Vδ2 T cell donors. Vγ9Vδ2 T cell ADCC capacity has also been linked to their differentiation state*(3)*, but transduction with either GFP-stIL15 or GFP-stIL15-14G2a had no effect on CD45RA or CD27 expression compared to

unmodified-γδ T cells, indicating no additional pressure towards terminal differentiation (fig. S9D).

Compared with freshly isolated γδ T cells, unmodified-γδ T cells, stIL15-γδ T cells and stIL15-14G2a-γδ T cells showed increased expression of the inflammatory homing chemokine receptors CCR2 and CXCR3, which are implicated in T cell infiltration of solid tumors*(32–34)* (Fig. 5D). stIL15-γδ T cells and 14G2a stIL15-OPS-γδ T cells also had increased CCR7 expression, potentially indicative of lymph node homing *(7, 32–36)*. Unmodified-γδ T cells and 14G2a stIL15-OPS-γδ T cells downregulated CXCR4, a receptor typically associated with tissue homing including to the bone marrow*(37)*. Chemokine expression profiles in transcriptomic data from 18 patient osteosarcoma samples were compared to patient-matched normal bone using DeSeq2 implemented in Python*(38)* (data from *(39)*, GEO accession GSE99671); 8 chemokines showed enhanced expression in osteosarcoma. Five of these chemokines matched with receptors that had enhanced expression in 14G2a stIL15-OPS-γδ T cells (CCL2, CXCL10, CXCL11, CCL13 and CCL19, Fig. 5E).

stIL15-OPS-γδ T cells have activity against osteosarcoma in vitro

To be translatable to clinic, 14G2a stIL15-OPS-γδ T cell immunotherapy must be manufacturable at scale and show activity against primary tumors exhibiting variable target antigen expression. Vγ9Vδ2 cell expansion, transducibility and viability were evaluated in scalable GMP-compatible G-Rex vessels. High product viability (>80%), purity (>90% Vδ2 cells of live cells) and transduction efficiency (>60%) were maintained

in this system. The cells were initiated at $2x10^6$ peripheral blood mononuclear cells (PBMCs)/cm^2, and yielded $11.7\pm2.8x10^6$ Vδ2 cells/cm^2 at harvest (12 days after initiation), corresponding to a total yield of approximately $5.6x10^9$ cells from a G-Rex 500M. Moreover, manufactured Vγ9Vδ2 T cells retained cytotoxic capacity (fig. S10).

Three patient-derived osteosarcoma lines*(40)* (kind gift from Dr Katia Scotlandi, Instituto Ortopedico Rizzoli, Bologna, Italy) were assessed for GD2 expression by flow cytometry (Fig. 6A), demonstrating variable and heterogenous expression similar to that which has been described clinically*(41)*. We evaluated the mechanism and efficacy of 14G2a stIL15-OPS-γδ T cell responses to osteosarcoma using a combination of 2D and 3D co-culture systems. Modelling of tumor-immune interactions in a 3D culture system provides an opportunity for more biomimetic culture that can be analyzed at single-cell resolution using CyTOF (fig. S11)*(42)*.

14G2a stIL15-OPS-γδ T cells in co-culture with osteosarcoma were compared to unmodified-γδ T cell monocultures using EMD to quantify differences in phospho-protein abundance. Baseline enhanced phosphorylation of key signaling nodes including ZAP70, AKT, and ERK in 14G2a stIL15-OPS-γδ T cells was preserved in the presence of PDOS19 and PDOS25, with an additional increase observed in pAKT and a reduction observed in pNFκB in response to GD2-expressing PDOS25, but not in response to GD2 negative PDOS19 (Fig. 6B and fig. S12A and B). Most target-induced effects were, however, GD2-autonomous, perhaps reflective of heterogenous expression of GD2 on PDOS25 and the multifactorial innate reactivity of stIL15-supported γδ T cells against tumor cells. Expression of perforin was higher in 14G2a stIL15-OPS-γδ T cells in the presence of osteosarcoma, and these target-induced increases were minimal or absent in unmodified-γδ T cells. Although co-culture with osteosarcoma cells slightly reduced the

519 abundance of pRb, pRb was still higher than in unmodified-γδ T cells in presence or
520 absence of tumor. Engineering with 14G2a stIL15-OPS was associated with reduced
521 pSTAT3 in the absence of targets, a pattern which was reversed in their presence (Fig.
522 6B and fig. S12A and B). Enhanced signal transducer and activator of transcription 3
523 (STAT3) signaling has previously been reported to confer resistance to activation-induced
524 cell death in γδ T cells*(43, 44)*; such effects would be consistent with the observed ability
525 of 14G2a stIL15-OPS-γδ T cells to persist and proliferate after repeatedly clearing tumor
526 challenge (Fig. 1H).

527 EMD analysis of osteosarcoma in coculture was performed relative to matched
528 osteosarcoma monocultures. Relative to tumor alone and tumor in co-culture with
529 unmodified-γδ T cells, 14G2a stIL15-OPS-γδ T cells induced substantial accumulation of
530 granzyme B in PDOS19 and upregulated cleaved PARP in both osteosarcoma 3D

cultures (Fig. 6C). The accumulation of perforin and granzyme B in the osteosarcoma is

Figure 6

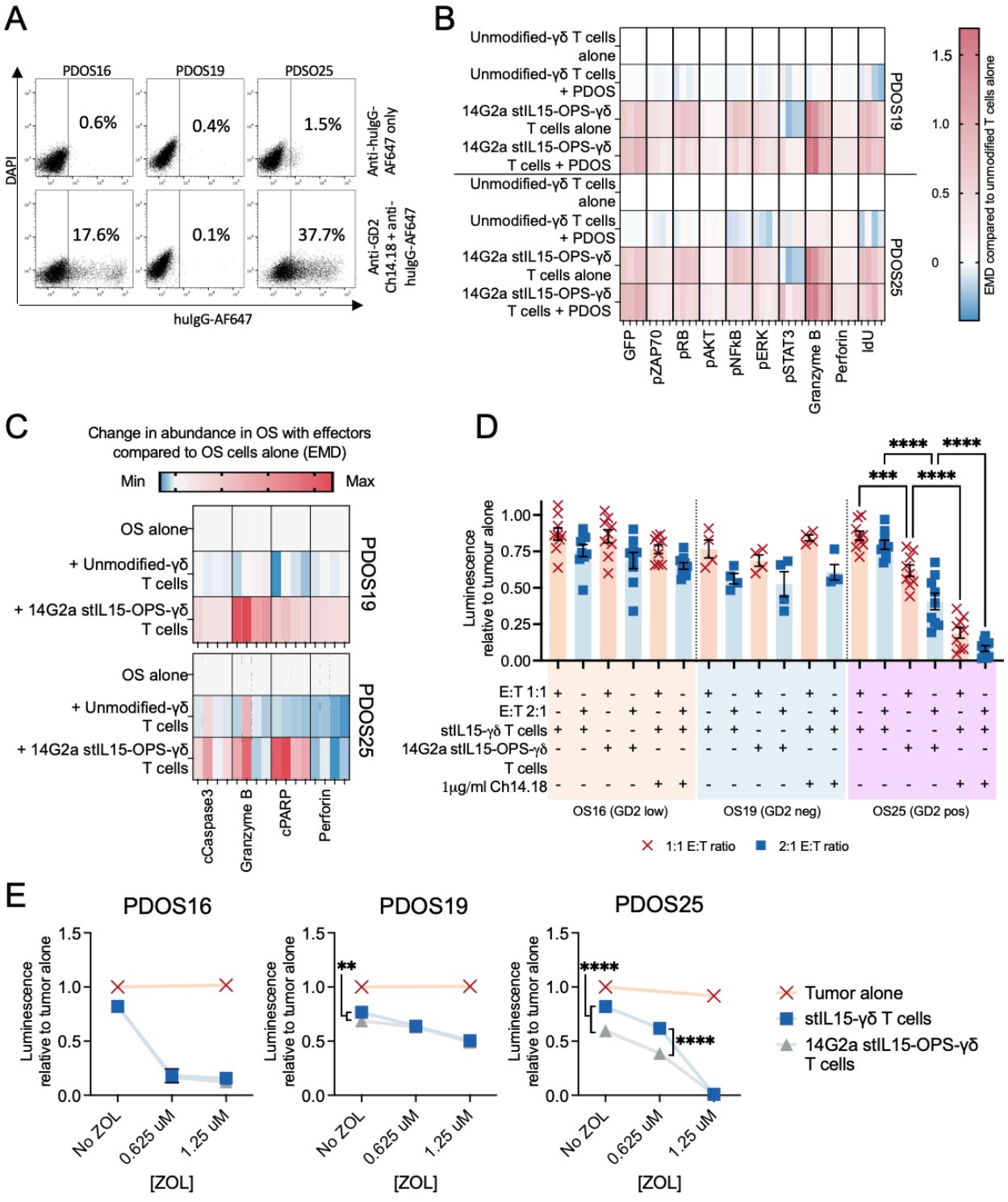

Figure 6: stIL15-OPS-γδ T cells display activity against primary osteosarcoma that can be maximized using zoledronic acid. (A) Expression of GD2 on 3 patient-derived OS lines: PDOS16, PDOS19 and PDOS25. **(B)** EMD analysis of signaling and functional

markers in unmodified-γδ or 14G2a stIL15-OPS-γδ T cells in the presence or absence of PDOS19 or PDOS25, using donor-matched unmodified-γδ T cells cultured alone as the baseline. **(C)** EMD analysis of cytolytic molecules and apoptotic markers in PDOS19 and PDOS25 in the presence or absence of either unmodified-γδ or 14G2a stIL15-OPS-γδ T cells, using osteosarcoma (OS) monoculture as the baseline. Data shown in all heatmaps in (B) and (C) is n=4 across 2 donors. **(D)** Quantification of luciferase-expressing PDOS lines in co-culture with stIL15-γδ or 14G2a stIL15-OPS-γδ T cells (n = 9 across 5 donors) at E:T ratios of 1:1 or 2:1 as measured by luminescence and plotted relative to tumor alone control. Individual data points and means ± SEM are shown, statistical comparisons are one-way ANOVA with Sidak's multiple comparison correction. **(E)** Same as (**D**), except tumor cells were pre-treated overnight with the indicated concentrations of zoledronic acid (ZOL) prior to co-culture with stIL15-γδ or 14G2a stIL15-OPS-γδ T cells at an E:T of 1:1 (means ± SEM are shown for n=12 across 4 donors). Effects were compared using a two-way repeated measures ANOVA with Sidak's multiple comparison correction. ***p<0.001, ****p<0.0001.

associated with increased presence of these effector molecules in co-cultured γδ T cells. Unmodified-γδ T cells led to reductions in osteosarcoma apoptotic markers including cleaved PARP and cleaved Caspase 3. To contextualize this information, we evaluated stIL15-γδ and stIL15-14G2a-engineered γδ T cell cytotoxicity against osteosarcoma in luminescence-based cytotoxicity assays. 14G2a stIL15-OPS-γδ T cells outperformed stIL15-γδ T cells at killing PDOS25, which had the highest GD2 expression and was also sensitive to ADCC induced by adding 1μg/mL Ch14.18 (Fig. 6D), but not PDOS16 and PDOS19. This innate responsiveness by unmodified-γδ T cells, stIL15-γδ T cells and 14G2a stIL15-OPS-γδ T cells could be augmented in vitro by pre-treating targets with zoledronic acid (Fig. 6E). Consistent with the ability of IL-15 to activate NK cells and recruit their ADCC capacity, supernatant from stIL15-γδ T cells enhanced the ability of fresh NK cells to kill PDOS25, a cytotoxic effect that was further boosted by 14G2a stIL15-OPS-γδ T cell supernatant (fig. S13).

stIL15-OPS-γδ T cells control osteosarcoma tumor burden in vivo

Accepting the limitations of modelling human γδ T cell immunotherapeutics in mice, we used an orthotopic patient-derived xenograft model to evaluate the ability of unmodified or engineered γδ T cells to control osteosarcoma growth in NSG mice. Following confirmation of successful intratibial engraftment of luciferase-expressing PDOS25 osteosarcoma cells, mice were randomized to different treatment groups (fig. S14) and administered a single $1x10^7$ intravenous dose of unmodified-γδ T cells, engineered γδ T cells or 14G2a 28ζ CAR-αβ T cells after tumor engraftment. 14G2a 28ζ CAR-αβ T cell validation is shown in fig. S15. Some animals further received a single dose of intraperitoneal zoledronic acid, Dinutuximab (Ch14.18) or both 7 days following cell therapy administration. No additional cytokine support was given to any of the animals.

No differences were observed in tumor luminescence between untreated animals and animals treated with zoledronic acid alone, Dinutuximab alone, or unmodified-γδ T cells with or without adjuvant zoledronic acid adjuvant treatment (Fig. 7A; event-free survival for selected groups is shown in Fig. 7B and for all the study groups in fig. S16A). Despite having previously demonstrated the capacity of stIL15 engineering to vastly boost γδ T cell persistence, stIL15-γδ T cells were no more efficacious against intratibial osteosarcoma than unmodified-γδ T cells. In contrast to unmodified-γδ T cells, however, stIL15-γδ T cell efficacy was enhanced by the co-administration of zoledronic acid, suggesting that the persisting stIL15-γδ T cell cytotoxicity can be favorably augmented with additional interventions. This was further demonstrated by a substantial increase in therapeutic efficacy when stIL15-producing γδ T cells also secreted 14G2a opsonin. Indeed, 14G2a stIL15-OPS-γδ T cell immunotherapy with zoledronic acid was as

efficacious against orthotopic osteosarcoma as stIL15-γδ T cell immunotherapy with zoledronic acid that was also treated with intravenous Dinutuximab (Fig. 7A), suggesting that γδ T cell-derived synthetic opsonin may mimic the exogenous addition of high-dose therapeutic antibody. The efficacy of stIL15-γδ T cells, zoledronic acid, and intravenous Dinutuximab was lost around day 60 after treatment, unlike 14G2a stIL15-OPS-γδ T and zoledronic acid, which continued to control tumor growth. Both treatments were more efficacious than validated 14G2a 28ζ CAR-αβ T cells that had killed PDOS25 in vitro (fig. S15C) but failed to control tumor burden in vivo (Fig. 7 and fig. S16A).

Using standardized scoring*(45)* (table S6), immunodeficient mice receiving 14G2a stIL15-OPS-γδ T cells showed no signs of neurotoxicity or allodynia, which has previously been reported with GD2 targeting immunotherapies using antibody clone 14G2a or its affinity enhanced variant 14G2a^{E101K}*(46, 47)*. Human IgG1 and human IL-15 will cross-react with murine receptors*(25, 46)*, but human γδ T would be rejected by an immunocompetent murine immune system, so we administered repeated doses of stIL15-γδ T cell 14G2a stIL15-OPS-γδ T cell supernatant to immunocompetent BALB/c mice to monitor for toxicity (fig. S16B). These mice remained healthy with no indication of ill

effects using the same standardized scoring systems, to the extent that toxicity scores remained at zero for all animals.

Figure 7

A

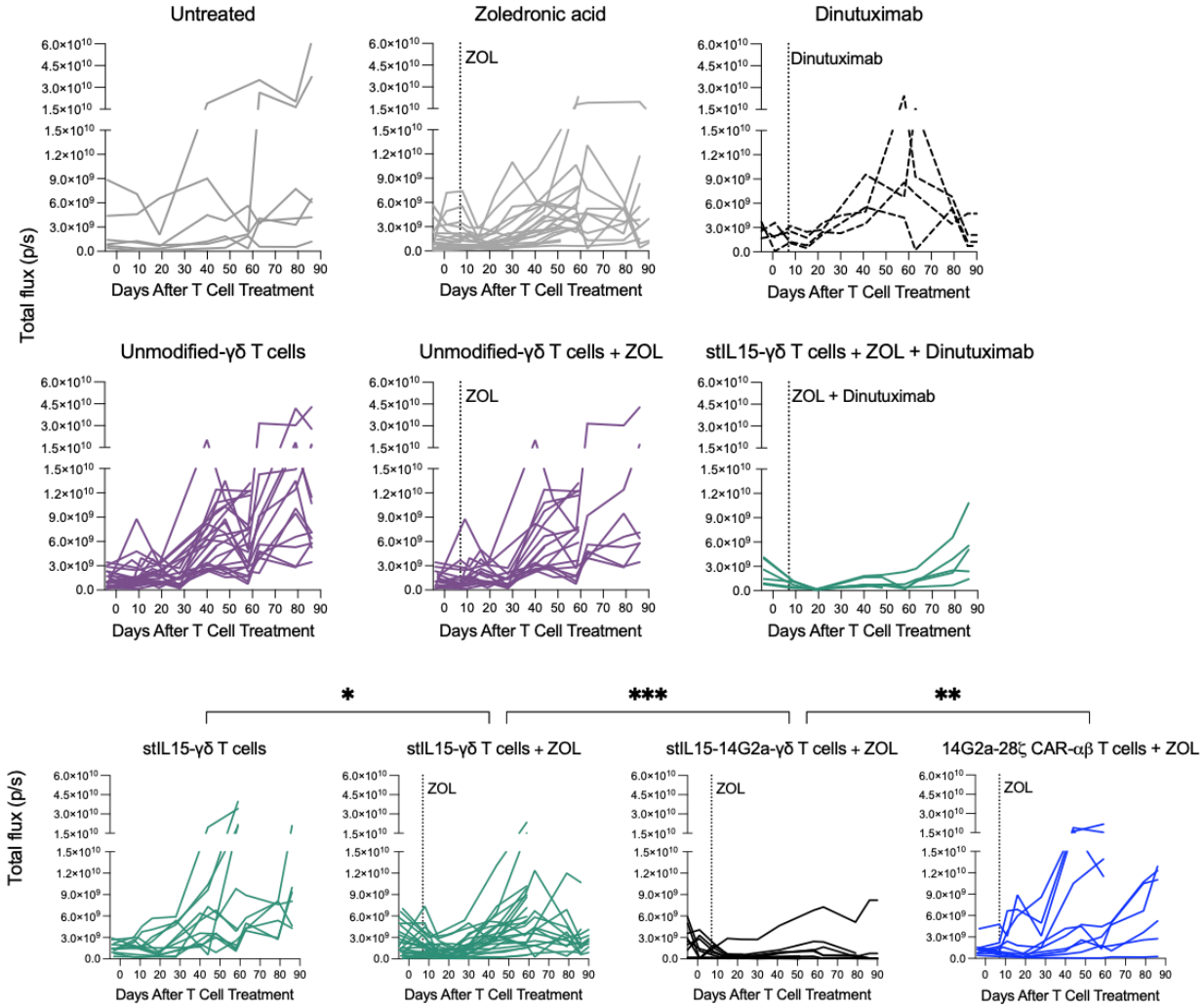

B

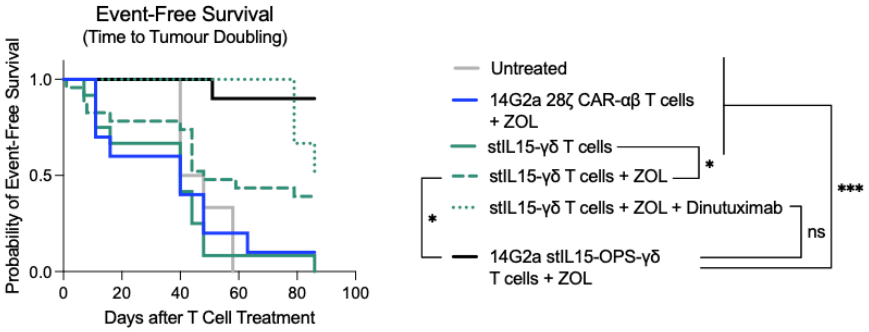

Figure 7: stIL15-OPS-γδ combined with zoledronic acid displays enhanced control of orthotopic primary osteosarcoma in vivo. NSG mice were given an intratibial injection of $0.5x10^6$ luciferase-expressing PDOS25 cells. After tumor engraftment, mice were infused with various T cell preparations by tail vein injection. 7 days after T cell infusion, some mice were given an intraperitoneal injection of ZOL (3μg/mouse), Dinutuximab (200μg/mouse), or both ZOL and Dinutuximab. The different treatment groups and their group sizes are as follows: Untreated (n=6), ZOL only (n=21), Dinutuximab only (n=4), unmodified-γδ (n=5), unmodified-γδ + ZOL (n=17), stIL15-γδ (n=12), stIL15-γδ + ZOL (n=23), stIL15-γδ + ZOL + Dinutuximab (n=6), 14G2a stIL15-OPS-γδ + ZOL (n=10), and 14G2a 28ζ CAR-αβ + ZOL (n=10). Blood samples were taken to track cell survival, and serial bioluminescence measurements were used to track tumor growth and efficacy over time. **(A)** Tumor growth curves for individual mice are plotted against time after T cell infusion. For statistical comparisons, linear regression then Brown-Forsythe and Welch ANOVA of slopes with Dunnett's T3 multiple comparison correction were used. **(B)** Event free survival was calculated as the time to progression, defined as a doubling in tumor bioluminescence and comparison of Kaplan Meier survival curves performed using the Mantel-Cox Log-rank test. ns, not significant; *p<0.05, **p<0.01, ***p<0.001.

DISCUSSION

Due to their safety in the allogeneic setting*(11, 47)*, γδ T cells have garnered increasing interest for their potential as cancer therapeutics*(11, 52).* Possessing innate and augmentable anti-tumor activity, they have entered the clinic in both unmodified and gene-modified formats. To date, the synthetic constructs used to boost γδ T cell immunotherapeutic potential in the clinic have been restricted to CARs that were previously developed for αβ T cells. This approach neglects the advantageous immunobiology of different γδ T cell subsets, which share properties of both T and NK cells*(48)*.

Here, we have described a combinatorial immunotherapeutic approach comprising γδ T cells engineered to secrete an IL-15 superagonist, stIL15, and a GD2-targeting scFv-Fc fusion protein opsonin. We have shown the effects of each of these components in isolation and provided a rationale for their combination, which outperformed binder-

matched traditional CAR-αβ therapy in orthotopic patient-derived osteosarcoma xenografts in vivo. Our approach represents a shift in synthetic engineering strategies; engineered OPS-γδ T cells extended enhancement of bystander cell cytotoxicity not only to unmodified γδ T cells, but also other antibody-based opsonin-engaging innate immune subsets, such as NK cells, macrophages, and neutrophils. By combining this cellular therapy with zoledronic acid, a well-characterized and licensed compound used in the treatment of bone-resident cancer*(49, 50)*, we further boosted therapeutic efficacy and introduced a bone-targeting mechanism that could be rapidly translated to the clinical setting.

With some notable exceptions, such as the recently demonstrated efficacy of GD2-targetting autologous CAR-αβ T in treating relapsed, refractory neuroblastoma*(51)*, the efficacy of cellular therapy against solid tumors has been limited. This remains a major unsolved bottleneck that iterative developments in CAR-T technology have not been successful in addressing. One of the purposes of the OPS-γδ T cell platform was to break away from reliance on membrane-bound enhancers of cytotoxicity. CAR T cell design evolved in the context of αβ T cells, where αβ TCR specificity against diverse MHC-presented epitopes must be bypassed using an alternative means of providing CD3 and costimulatory signals upon encountering tumor. Unconstrained by this restriction due to their MHC-independent recognition of butyrophillins*(52, 53)* as a means of detecting transformed cells*(54)*, Vγ9Vδ2 cells do not require the inclusion of a CD3ζ motif in membrane-bound constructs*(28, 55)*. We have now demonstrated that they do not require membrane-bound enhancers to boost their cytotoxicity at all. The ability of the Vγ9Vδ2 γδ T cell subset to exert ADCC has been extensively documented by us *(5, 6)* and others *(3, 4, 31)*. Antibody or bispecific T cell engager (BiTE) payload delivery from engineered αβ T cells has been described previously*(56–58)*, though the contribution of these payloads

669 to ADCC was relatively unexplored, in part because αβT cells lack this innate immune
670 capability.

671 From a manufacturing and delivery perspective, the most striking difference
672 afforded through using γδ T cells as the T cell substrate is the ability to pre-manufacture
673 an allogeneic product and generate off-the-shelf cell therapies, resulting in a marked
674 reduction in production costs. This has been addressed to an extent by the generation of
675 CAR-γδ T cell approaches. CAR-γδ T cells are showing some promise in the clinic*(47)*
676 and are the topic of a number of successful preclinical studies *(59)*. However, the inherent
677 limitations of CAR technology, including tonic signaling, on-target off-tumor toxicity and
678 lack of microenvironmental engagement, remain. In accordance with previous studies *(28,*
679 *60, 61)*, CAR constructs, in this case those bearing CD3ζ and CD28 endodomains,
680 exhibited evidence of tonic signaling that manifested as CAR-dependent increases in
681 phosphorylation of moieties downstream of CD3ζ and was accompanied by increased
682 expression of checkpoint receptors TIM-3, LAG-3 and TIGIT.

683 In this study and previously*(5, 6)* we have linked Vγ9Vδ2 antibody-dependent
684 cytotoxicity to expression of CD16 and observed a switch from a predominantly CD16b
685 expressing phenotype to more stimulatory CD16a expression in 14G2a OPS-γδ T cells
686 compared to unmodified-γδ T cells. CD16 expression has recently gained some
687 prominence as a biomarker of Vγ9Vδ2 T cell cytotoxicity*(31)*, although perhaps
688 unsurprisingly, in the absence of opsonin, Vγ9Vδ2 T cells engineered to express higher
689 CD16a did not show higher cytotoxicity in an ovarian cancer model, suggesting that
690 natural CD16 expression is indicative of effector programming rather than regulating
691 opsonin-independent function. Expression of stIL15 or 14G2a stIL15-OPS constructs had
692 no effect on total CD16 expression in Vγ9Vδ2 T cells, nor on γδ T cell CD45RA/CD27
693 expression, which have also been linked to ADCC effector function as markers of T cell

differentiation *(3)*. These data suggest that the pre-expansion CD16 phenotype could be used as a donor-screening metric. Beyond the Vγ9Vδ2 T cell preparation itself, evidence of bystander engagement in our simple in vitro models suggests that factors governing stIL15-OPS-γδ T cell efficacy will not reside solely with the cell therapy product. This is important, as engagement of opsonized target cells does not lead to an accelerated proliferative response in engineered cells, unlike the responses seen with CARs in αβ T cells or γδ T cells and chimeric costimulatory receptors in γδ T cells*(28)*.

It is well recognized that solid tumors pose a major challenge for the trafficking of cellular immunotherapeutics, and especially so in the context of bone-resident disease*(62)*. OPS-γδ T cells were designed to overcome this challenge, as Vγ9Vδ2 T cell homing can be modulated using hydroxy apatite-binding and FDA-approved bisphosphonate compounds like zoledronic acid, which can also act as a potent sensitizer of cancer cells to Vγ9Vδ2 T cell cytotoxicity. Acting in an indirect manner by blocking part of the mevalonate pathway of cholesterol biosynthesis, with resultant increases in intracellular isopentenyl-5-pyrophosphate and conformational changes in the Vγ9Vδ2 TCR-engaging butyrophillin, bisphosphonates are used in many Vγ9Vδ2 T cell expansion protocols, including our own. Following administration to adult patients, 62±13% of a 4 mg zoledronic acid dose binds to the bone, and the rest is excreted unchanged*(63)*, making the co-administration of zoledronic acid with γδ T cells of particular interest for targeting bone-resident disease. This was used to good effect in a recently published combination with CAR-γδ T cells to treat bony disease in a murine xenograft model of prostate cancer*(59)*. This context-specific synergy informed our choice to include it in the in vivo experiments targeting osteosarcoma, having already demonstrated that 14G2a stIL15-OPS-γδ T cells were efficacious in the subcutaneous model without zoledronic acid.

Zoledronic acid was required for stIL15-γδ T cell immunotherapy to slow orthotopic patient-derived osteosarcoma growth, but the efficacy of combined 14G2a stIL15-OPS-γδ T cells with zoledronic acid was such that tumors failed to grow and indeed decreased in size in 8 of 10 animals following a single T cell administration, which was maintained over the three-month duration of the study. This was not observed following a single dose of 14G2a binder-matched 2nd generation CAR-αβ T cells, which provided no benefit. A similar therapeutic effect could be achieved by combining stIL15-γδ T cellular immunotherapy and zoledronic acid and a single high dose of intravenous Dinutuximab, but only transiently. This points to the high therapeutic value of combining stIL15-armoured Vγ9Vδ2 T cellular immunotherapy with GD2-targeting ADCC mediators and zoledronic acid but underscores that a continuous supply of opsonin may be required for continued efficacy.

Due to the challenges of immunohistochemical analysis of heavily calcified tumors it has not been possible to interrogate the tumor immune infiltrate, but the chemokine and chemokine receptor profiling, coupled with the efficacy data, provide evidence in support of tumor homing. Furthermore, our mechanistic data suggests that 14G2a stIL15-OPS-γδ T cells are resistant to the suppressive effects of osteosarcoma in 3D culture models, unlike unmodified-γδ T cells, which presented with impaired cell cycling (as evidenced by reduced IdU incorporation) and failed to control aggressive osteosarcoma growth in vitro and in vivo.

There are limitations to our study, derived in part from the T cell type under investigation. In demonstrating the efficacy of a potential therapeutic product, we minimized additional handling steps applied to the engineered cells. This leads to slight inter-batch variability in γδT cell content and transduction which could impact the consistency of results. The reliance of OPS-γδ T cell immunotherapy on natural

mechanisms of cytotoxicity is a potential limitation of the approach, given the variable expression of Fcγ receptors on Vγ9Vδ2 cells. Deeper characterization of CD16 polymorphisms with influence on Fc binding may further clarify the role of the CD16-opsonin interaction. Modelling the efficacy of our engineered γδ T cell product in vivo is, by necessity, artificial. γδ T cells in mice and humans are profoundly different, precluding immunocompetent mouse modelling and thus full engagement of immune bystanders which we anticipate may be recruited by opsonin and stIL15.

Our finding that un-engineered γδT cells in autologous or allogeneic contexts are ineffective is in accordance with those of others*(64)*, a limitation not restricted to the Vγ9Vδ2 subset*(65)*. In our models, reduced apoptotic and increased proliferative signals were observed in osteosarcoma co-cultured with un-engineered γδ T cells. This contributes to evolving evidence indicating that highly expanded un-engineered γδ T cells may promote tumor growth, a key limitation which must be explored further.

Here, we demonstrate that Vγ9Vδ2 T cells engineered to secrete an IL-15 receptor super-agonist and an anti-GD2 opsonin can harness synergy with aminobisphosphonates to control osteosarcoma in vivo. These results provide a strong rationale for the use of this combinatorial cell therapy approach to treat bone-resident cancers. Having demonstrated superiority over conventional CAR-αβ T cell-based therapies, both in terms of efficacy and potential for allogeneic, off the shelf delivery, there is now a need for further developments targeting more ubiquitously expressed tumor-associated antigens and extra-osseous, metastatic disease in order to maximize patient benefit.

MATERIALS AND METHODS

Study design

This study's primary research objective is proof-of-concept for a allogeneic cell-based therapy specifically designed for solid tumor targeting. The therapy comprises Vγ9Vδ2 γδ T cells engineered to secrete ADCC- and ADCP-inducing tumor-targeting opsonins in combination with a cytokine-based mitogen. As this therapy is allogeneic, and can be generated from pre-validated donor material, we designed experiments using γδ T cells sourced from healthy donor blood. We observed a strong correlation between Vγ9Vδ2 ADCC efficacy and the amount of CD16 on their surface. In keeping with a proposed "off the shelf" immunotherapeutic, we therefore preselected donors whose Vγ9Vδ2 T cells expressed high amounts of CD16 for this study. Healthy donor bystander cells were used to demonstrate recruitment of non-engineered immune cells and to model potential interactions with the patient's own immune system. A range of relevant in vitro and in vivo assessments were used to test the feasibility and efficacy of this platform technology, and different techniques including flow cytometry, mass cytometry, and ELISA, were employed to interrogate the immune-tumor interactome. To model the tumor, we used both primary tumor lines and isogenic cell lines with engineered GD2 expression. 2D and 3D in vitro experiments were conducted in both experimental and biological replicates for sufficient statistical power; specific details for the value of n are provided in the figure legends for individual experiments. For our in vivo model, a study was initially conducted with 3 mice per group to inform safety and power calculations, and then repeated with larger group sizes of 6 mice per group. Statistical analyses were performed on complete expanded data sets incorporating both experimental and biological replicates. Investigators were not blinded during experimental setup or sample acquisition, and no outliers were excluded from the datasets presented. This study was approved by a national ethics committee (West Midlands HRA, 14/WM/1253) and complied with the

WMA declaration of Helsinki. Tabulated data files for this study are available on Dryad (https://doi.org/10.5061/dryad.q2bvq83t1).

Statistical analyses

All statistical analyses were performed using GraphPad Prism 9.3.0. P values of less than 0.05 were considered statistically significant. *, **, ***, and **** were used to indicate p values of <0.05, <0.01, <0.001 and <0.0001, respectively in the figures. Normalcy of data distribution was determined by Shapiro-Wilk testing. Where two normally distributed groups of values were compared, paired or unpaired t-tests were used. If more than two normally distributed groups were compared, one-way or two-way ANOVA with Sidak's or Tukey's multiple comparison correction was used to determine differences between groups. Comparison of non-normally distributed data was carried out using the non-parametric Mann-Whitney test (for unpaired comparisons of two groups) or Kruskal-Wallis test with Dunn's multiple comparison correction (for comparisons of more than one group). For differential expression analysis of previously published transcriptomic data, the Python implementation of deseq2 (PyDeseq2 *(38)*) was used. In-vivo osteosarcoma growth kinetics were determined using simple linear regression, using each biological replicate as an individual data point. Tumor growth was then compared using Brown-Forsyth and Welch ANOVA with Dunnett's T3 multiple comparison correction. Osteosarcoma event-free survival was determined by defining an "event" as doubling of tumor bioluminescence compared to baseline. Where other analyses have been used, details are given in the appropriate legend.

Supplemental Materials

Supplemental Materials and Methods

Fig. S1 to S16

Tables S1 to S6

MDAR Reproducibility Checklist

References

1. J. J. Melenhorst, G. M. Chen, M. Wang, D. L. Porter, C. Chen, M. A. Collins, P. Gao, S. Bandyopadhyay, H. Sun, Z. Zhao, S. Lundh, I. Pruteanu-Malinici, C. L. Nobles, S. Maji, N. V Frey, S. I. Gill, L. Tian, I. Kulikovskaya, M. Gupta, D. E. Ambrose, M. M. Davis, J. A. Fraietta, J. L. Brogdon, R. M. Young, A. Chew, B. L. Levine, D. L. Siegel, C. Alanio, E. J. Wherry, F. D. Bushman, S. F. Lacey, K. Tan, C. H. June, Decade-long leukaemia remissions with persistence of CD4+ CAR T cells. *Nature* **602**, 503–509 (2022).
2. M. Sadelain, I. Rivière, S. Riddell, Therapeutic T cell engineering. *Nature* **545**, 423 431.
3. D. F. Angelini, G. Borsellino, M. Poupot, A. Diamantini, R. Poupot, G. Bernardi, F. Poccia, J.-J. Fournié, L. Battistini, FcγRIII discriminates between 2 subsets of Vγ9Vδ2 effector cells with different responses and activation pathways. *Blood* **104**, 1801–1807.
4. J. Gertner-Dardenne, C. Bonnafous, C. Bezombes, A.-H. Capietto, V. Scaglione, S. Ingoure, D. Cendron, E. Gross, J.-F. Lepage, A. Quillet-Mary, L. Ysebaert, G. Laurent, H. Sicard, J.-J. Fournié, Bromohydrin pyrophosphate enhances antibody-dependent cell-mediated cytotoxicity induced by therapeutic antibodies. *Blood* **113**, 4875–4884.
5. J. P. H. Fisher, B. Flutter, F. Wesemann, J. Frosch, C. Rossig, K. Gustafsson, J. Anderson, Effective combination treatment of GD2-expressing neuroblastoma and Ewing's sarcomausing anti-GD2 ch14.18/CHO antibody with Vγ9Vδ2+γδT cells. *Oncoimmunology* **5** (2016), doi:10.1080/2162402X.2015.1025194.
6. J. P. H. Fisher, M. Yan, J. Heuijerjans, L. Carter, A. Abolhassani, J. Frosch, R. Wallace, B. Flutter, A. Capsomidis, M. Hubank, N. Klein, R. Callard, K. Gustafsson, J. Anderson, Neuroblastoma killing properties of Vδ2 and Vδ2-negative γδT cells following expansion by artificial antigen-presenting cells. *Clinical Cancer Research* **20** (2014), doi:10.1158/1078-0432.CCR-13-3464.
7. C. J. Tyler, N. E. McCarthy, J. O. Lindsay, A. J. Stagg, B. Moser, M. Eberl, Antigen-Presenting Human γδ T Cells Promote Intestinal CD4(+) T Cell Expression of IL-22 and Mucosal Release of Calprotectin. *J Immunol* **198**, 3417–3425 (2017).
8. G. Pizzolato, H. Kaminski, M. Tosolini, D.-M. Franchini, F. Pont, F. Martins, C. Valle, D. Labourdette, S. Cadot, A. Quillet-Mary, M. Poupot, C. Laurent, L. Ysebaert, S. Meraviglia, F. Dieli, P. Merville, P. Milpied, J. Déchanet-Merville, J.-J. Fournié, Single-cell RNA sequencing unveils the shared and the distinct cytotoxic hallmarks of human TCRVδ1 and TCRVδ2 γδ T lymphocytes. *Proceedings of the National Academy of Sciences* , 201818488 (2019).
9. D. C. Deniger, K. Switzer, T. Mi, S. Maiti, L. Hurton, H. Singh, H. Huls, S. Olivares, D. A. Lee, R. E. Champlin, L. J. Cooper, Bispecific T-cells Expressing Polyclonal Repertoire of Endogenous γδ T-cell Receptors and Introduced CD19-specific Chimeric Antigen Receptor. *Mol Ther* **21**, 638 647.
10. D. C. Deniger, S. N. Maiti, T. Mi, K. C. Switzer, V. Ramachandran, L. V Hurton, S. Ang, S. Olivares, B. A. Rabinovich, M. H. Huls, D. A. Lee, R. C. Bast, R. E. Champlin, L. J. N. Cooper, Activating and Propagating Polyclonal Gamma Delta T Cells with Broad Specificity for Malignancies. *Clinical Cancer Research* **20**, 5708–5719.
11. Y. Xu, Z. Xiang, M. Alnaggar, L. Kouakanou, J. Li, J. He, J. Yang, Y. Hu, Y. Chen, L. Lin, J. Hao, J. Li, J. Chen, M. Li, Q. Wu, C. Peters, Q. Zhou, J. Li, Y. Liang, X. Wang, B. Han, M. Ma, D. Kabelitz, K. Xu, W. Tu, Y. Wu, Z. Yin, Allogeneic Vγ9Vδ2 T-cell immunotherapy exhibits promising clinical safety and prolongs the survival of patients with late-stage lung or liver cancer. *Cell Mol Immunol* **18**, 427–439 (2021).
12. A. J. Gentles, A. M. Newman, C. L. Liu, S. V Bratman, W. Feng, D. Kim, V. S. Nair, Y. Xu, A. Khuong, C. D. Hoang, M. Diehn, R. B. West, S. K. Plevritis, A. A. Alizadeh, The prognostic landscape of genes and infiltrating immune cells across human cancers. *Nat Med* **21**, 938 945.
13. J. H. Park, H.-J. Kim, C. W. Kim, H. C. Kim, Y. Jung, H.-S. Lee, Y. Lee, Y. S. Ju, J. E. Oh, S.-H. Park, J. H. Lee, S. K. Lee, H. K. Lee, Tumor hypoxia represses γδ T cell-mediated antitumor immunity against brain tumors. *Nat Immunol* **22**, 336–346 (2021).
14. J. Theruvath, M. Menard, B. A. H. Smith, M. H. Linde, G. L. Coles, G. N. Dalton, W. Wu, L. Kiru, A. Delaidelli, E. Sotillo, J. L. Silberstein, A. C. Geraghty, A. Banuelos, M. T. Radosevich, S. Dhingra, S. Heitzeneder, A. Tousley, J. Lattin, P. Xu, J. Huang, N. Nasholm, A. He, T. C. Kuo, E. R. B. Sangalang, J. Pons, A. Barkal, R. E. Brewer, K. D. Marjon, J. G. Vilches-Moure, P. L. Marshall, R. Fernandes, M. Monje, J. R. Cochran, P. H. Sorensen, H. E. Daldrup-Link, I. L. Weissman, J. Sage, R. Majeti, C. R. Bertozzi, W. A. Weiss, C. L. Mackall, R. G. Majzner, Anti-GD2 synergizes with CD47 blockade to mediate tumor eradication. *Nat Med* **28**, 333–344 (2022).
15. R. Ladenstein, U. Pötschger, D. Valteau-Couanet, R. Luksch, V. Castel, I. Yaniv, G. Laureys, P. Brock, J. M. Michon, C. Owens, T. Trahair, G. C. F. Chan, E. Ruud, H. Schroeder, M. B. Popovic, G. Schreier, H. Loibner, P. Ambros, K. Holmes, M. R. Castellani, M. N. Gaze, A. Garaventa, A. D. J. Pearson, H. N. Lode, Interleukin 2 with anti-GD2 antibody ch14.18/CHO (dinutuximab beta) in patients with high-risk neuroblastoma (HR-NBL1/SIOPEN): a multicentre, randomised, phase 3 trial. *Lancet Oncol* **19**, 1617–1629 (2018).
16. P. Hingorani, M. D. Krailo, A. Buxton, P. R. Hutson, J. Davis, K. A. Janeway, R. G. Gorlick, M. Isakoff, Phase II study of antidisialoganglioside antibody, dinutuximab, in combination with GM-CSF in patients with recurrent

osteosarcoma (AOST1421): A report from the Children's Oncology Group. *Journal of Clinical Oncology* **38**, 10508–10508 (2020).
17. M. Roth, M. Linkowski, J. Tarim, S. Piperdi, R. Sowers, D. Geller, J. Gill, R. Gorlick, Ganglioside GD2 as a therapeutic target for antibody-mediated therapy in patients with osteosarcoma. *Cancer* **120**, 548–54 (2013).
18. A. R. M. Almeida, D. V Correia, A. Fernandes-Platzgummer, C. L. da Silva, M. G. da Silva, D. R. Anjos, B. Silva-Santos, Delta One T cells for immunotherapy of chronic lymphocytic leukemia: clinical-grade expansion/ differentiation and preclinical proof-of-concept. *American Association for Cancer Research* **22**, clincanres.0597.2016 (2016).
19. G. M. Ferry, C. Agbuduwe, M. Forrester, S. Dunlop, K. Chester, J. Fisher, J. Anderson, M. Barisa, A Simple and Robust Single-Step Method for CAR-Vδ1 γδT Cell Expansion and Transduction for Cancer Immunotherapy. *Front Immunol* **13** (2022), doi:10.3389/fimmu.2022.863155.
20. H. H. Van Acker, S. Anguille, Y. Willemen, J. M. Van den Bergh, Z. N. Berneman, E. Lion, E. L. Smits, V. F. Van Tendeloo, Interleukin-15 enhances the proliferation, stimulatory phenotype, and antitumor effector functions of human gamma delta T cells. *J Hematol Oncol* **9**, 101 (2016).
21. A. Makkouk, X. (Cher) Yang, T. Barca, A. Lucas, M. Turkoz, J. T. S. Wong, K. P. Nishimoto, M. M. Brodey, M. Tabrizizad, S. R. Y. Gundurao, L. Bai, A. Bhat, Z. An, S. Abbot, D. Satpayev, B. T. Aftab, M. Herrman, Off-the-shelf Vδ1 gamma delta T cells engineered with glypican-3 (GPC-3)-specific chimeric antigen receptor (CAR) and soluble IL-15 display robust antitumor efficacy against hepatocellular carcinoma. *J Immunother Cancer* **9**, e003441 (2021).
22. M. Desbois, C. Béal, M. Charrier, B. Besse, G. Meurice, N. Cagnard, Y. Jacques, D. Béchard, L. Cassard, N. Chaput, IL-15 superagonist RLI has potent immunostimulatory properties on NK cells: implications for antimetastatic treatment. *J Immunother Cancer* **8**, e000632 (2020).
23. K. Han, X. Zhu, B. Liu, E. Jeng, L. Kong, J. L. Yovandich, V. V Vyas, W. D. Marcus, P.-A. Chavaillaz, C. A. Romero, P. R. Rhode, H. C. Wong, IL-15:IL-15 receptor alpha superagonist complex: High-level co-expression in recombinant mammalian cells, purification and characterization. *Cytokine* **56**, 804–810 (2011).
24. E. Mortier, A. Quéméner, P. Vusio, I. Lorenzen, Y. Boublik, J. Grötzinger, A. Plet, Y. Jacques, Soluble Interleukin-15 Receptor α (IL-15Rα)-sushi as a Selective and Potent Agonist of IL-15 Action through IL-15Rβ/γ HYPERAGONIST IL-15·IL-15Rα FUSION PROTEINS. *Journal of Biological Chemistry* **281**, 1612–1619 (2006).
25. Y. Guo, L. Luan, N. K. Patil, E. R. Sherwood, Immunobiology of the IL-15/IL-15Rα complex as an antitumor and antiviral agent. *Cytokine Growth Factor Rev* **38**, 10–21 (2017).
26. K. M. Knudson, J. W. Hodge, J. Schlom, S. R. Gameiro, Rationale for IL-15 superagonists in cancer immunotherapy. *Expert Opin Biol Ther* **20**, 1–5 (2020).
27. J. Feng, H. Xu, A. Cinquina, Z. Wu, Q. Chen, P. Zhang, X. Wang, H. Shan, L. Xu, Q. Zhang, L. Sun, W. Zhang, K. G. Pinz, M. Wada, X. Jiang, W. M. Hanes, Y. Ma, H. Zhang, Treatment of Aggressive T Cell Lymphoblastic Lymphoma/leukemia Using Anti-CD5 CAR T Cells. *Stem Cell Rev Rep* **17**, 652–661 (2021).
28. J. Fisher, R. Sharma, D. W. Don, M. Barisa, M. O. Hurtado, P. Abramowski, L. Porter, W. Day, R. Borea, S. Inglott, J. Anderson, D. Pe'er, Engineering γδT cells limits tonic signaling associated with chimeric antigen receptors. *Sci Signal* **12**, eaax1872 (2019).
29. S. Krishnaswamy, M. H. Spitzer, M. Mingueneau, S. C. Bendall, O. Litvin, E. Stone, D. Pe'er, G. P. Nolan, Conditional density-based analysis of T cell signaling in single-cell data. *Science (1979)* **346**, 1250689.
30. J. Dunne, S. Lynch, C. O'Farrelly, S. Todryk, J. E. Hegarty, C. Feighery, D. G. Doherty, Selective Expansion and Partial Activation of Human NK Cells and NK Receptor-Positive T Cells by IL-2 and IL-15. *The Journal of Immunology* **167**, 3129–3138 (2001).
31. D. Lee, Z. S. Dunn, W. Guo, C. J. Rosenthal, N. E. Penn, Y. Yu, K. Zhou, Z. Li, F. Ma, M. Li, T.-C. Song, X. Cen, Y.-R. Li, J. J. Zhou, M. Pellegrini, P. Wang, L. Yang, Unlocking the potential of allogeneic Vδ2 T cells for ovarian cancer therapy through CD16 biomarker selection and CAR/IL-15 engineering. , doi:10.1038/s41467-023-42619-2.
32. N. Himoudi, D. A. Morgenstern, M. Yan, B. Vernay, L. Saraiva, Y. Wu, C. J. Cohen, K. Gustafsson, J. Anderson, Human γδ T Lymphocytes Are Licensed for Professional Antigen Presentation by Interaction with Opsonized Target Cells. *The Journal of Immunology* **188**, 1708–1716.
33. J. Anderson, K. Gustafsson, N. Himoudi, M. Yan, J. Heuijerjans, Licensing of γδT cells for professional antigen presentation. *Oncoimmunology* **1**, 1652–1654.
34. A. Capsomidis, G. Benthall, H. H. Van Acker, J. Fisher, A. M. Kramer, Z. Abeln, Y. Majani, T. Gileadi, R. Wallace, K. Gustafsson, B. Flutter, J. Anderson, Chimeric Antigen Receptor-Engineered Human Gamma Delta T Cells: Enhanced Cytotoxicity with Retention of Cross Presentation. *Molecular Therapy* **26** (2018), doi:10.1016/j.ymthe.2017.12.001.
35. M. Brandes, K. Willimann, B. Moser, Professional Antigen-Presentation Function by Human γδ T Cells. *Science (1979)* **309**, 264–268.
36. B. Moser, M. Eberl, γδ T-APCs: a novel tool for immunotherapy? *Cell Mol Life Sci* **68**, 2443 2452.

37. K. M. Ramonell, W. Zhang, A. Hadley, C. Chen, K. T. Fay, J. D. Lyons, N. J. Klingensmith, K. W. McConnell, C. M. Coopersmith, M. L. Ford, CXCR4 blockade decreases CD4+ T cell exhaustion and improves survival in a murine model of polymicrobial sepsis. *PLoS One* **12**, e0188882 (2017).
38. B. Muzellec, M. Teleńczuk, V. Cabeli, M. Andreux, PyDESeq2: a python package for bulk RNA-seq differential expression analysis. *bioRxiv* , 2022.12.14.520412 (2022).
39. X. D. Ho, P. Phung, V. Q. Le, V. H. Nguyen, E. Reimann, E. Prans, G. Kõks, K. Maasalu, N. T. N. Le, L. H. Trinh, H. G. Nguyen, A. Märtson, S. Kõks, Whole transcriptome analysis identifies differentially regulated networks between osteosarcoma and normal bone samples. *Exp Biol Med* **242**, 1802–1811 (2017).
40. P. Nanni, L. Landuzzi, M. C. Manara, A. Righi, G. Nicoletti, C. Cristalli, M. Pasello, A. Parra, M. Carrabotta, M. Ferracin, A. Palladini, M. L. Ianzano, V. Giusti, F. Ruzzi, M. Magnani, D. M. Donati, P. Picci, P.-L. Lollini, K. Scotlandi, Bone sarcoma patient-derived xenografts are faithful and stable preclinical models for molecular and therapeutic investigations. *Sci Rep* **9**, 12174 (2019).
41. B. Nazha, C. Inal, T. K. Owonikoko, Disialoganglioside GD2 Expression in Solid Tumors and Role as a Target for Cancer Therapy. *Front Oncol* **10**, 1000 (2020).
42. X. Qin, J. Sufi, P. Vlckova, P. Kyriakidou, S. E. Acton, V. S. W. Li, M. Nitz, C. J. Tape, Cell-type-specific signaling networks in heterocellular organoids. *Nat Methods* , 1–8 (2020).
43. J. H. Park, H. K. Lee, Function of γδ T cells in tumor immunology and their application to cancer therapy. *Exp Mol Med* **53**, 318–327 (2021).
44. M.-L. Michel, D. J. Pang, S. F. Y. Haque, A. J. Potocnik, D. J. Pennington, A. C. Hayday, Interleukin 7 (IL-7) selectively promotes mouse and human IL-17–producing γδ cells. *Proceedings of the National Academy of Sciences* **109**, 17549–17554 (2012).
45. D. J. Langford, A. L. Bailey, M. L. Chanda, S. E. Clarke, T. E. Drummond, S. Echols, S. Glick, J. Ingrao, T. Klassen-Ross, M. L. LaCroix-Fralish, L. Matsumiya, R. E. Sorge, S. G. Sotocinal, J. M. Tabaka, D. Wong, A. M. J. M. van den Maagdenberg, M. D. Ferrari, K. D. Craig, J. S. Mogil, Coding of facial expressions of pain in the laboratory mouse. *Nat Methods* **7**, 447–449 (2010).
46. M. B. Overdijk, S. Verploegen, A. O. Buijsse, T. Vink, J. H. W. Leusen, W. K. Bleeker, P. W. H. I. Parren, Crosstalk between Human IgG Isotypes and Murine Effector Cells. *The Journal of Immunology* **189**, 3430–3438.
47. S. S. Neelapu, M. Hamadani, D. B. Miklos, H. Holmes, J. Hinkle, J. Kennedy-Wilde, O. Maller, M. Weinstein, F. Galimi, R. Lai, D. A. Stevens, A phase 1 study of ADI-001: Anti-CD20 CAR-engineered allogeneic gamma delta (γδ) T cells in adults with B-cell malignancies. *Journal of Clinical Oncology* **40**, 7509–7509 (2022).
48. S. Mensurado, R. Blanco-Domínguez, B. Silva-Santos, The emerging roles of γδ T cells in cancer immunotherapy. *Nat Rev Clin Oncol* **20**, 178–191 (2023).
49. J.-P. Lorange, J. Ramirez, G. Luna, F. Grou-Boileau, D. Rosenzweig, M. H. Weber, E. Akoury, Management of bone metastasis with zoledronic acid: A systematic review and Bayesian network meta-analysis. *J BONE ONCOL* **39**, 100470 (2023).
50. S. Piperno-Neumann, M.-C. Le Deley, F. Rédini, H. Pacquement, P. Marec-Bérard, P. Petit, H. Brisse, C. Lervat, J.-C. Gentet, N. Entz-Werlé, A. Italiano, N. Corradini, E. Bompas, N. Penel, M.-D. Tabone, A. Gomez-Brouchet, J.-M. Guinebretière, E. Mascard, F. Gouin, A. Chevance, N. Bonnet, J.-Y. Blay, L. Brugières, S. G. of UNICANCER, F. S. of P. O. (SFCE), F. S. G. (GSF-GETO), Zoledronate in combination with chemotherapy and surgery to treat osteosarcoma (OS2006): a randomised, multicentre, open-label, phase 3 trial. *Lancet Oncol* **17**, 1070–1080 (2016).
51. F. Del Bufalo, B. De Angelis, I. Caruana, G. Del Baldo, M. A. De Ioris, A. Serra, A. Mastronuzzi, M. G. Cefalo, D. Pagliara, M. Amicucci, G. Li Pira, G. Leone, V. Bertaina, M. Sinibaldi, S. Di Cecca, M. Guercio, Z. Abbaszadeh, L. Iaffaldano, M. Gunetti, S. Iacovelli, R. Bugianesi, S. Macchia, M. Algeri, P. Merli, F. Galaverna, R. Abbas, M. C. Garganese, M. F. Villani, G. S. Colafati, F. Bonetti, M. Rabusin, K. Perruccio, V. Folsi, C. Quintarelli, F. Locatelli, GD2-CART01 for Relapsed or Refractory High-Risk Neuroblastoma. *New England Journal of Medicine* **388**, 1284–1295 (2023).
52. S. Vavassori, A. Kumar, G. S. Wan, G. S. Ramanjaneyulu, M. Cavallari, S. El Daker, T. Beddoe, A. Theodossis, N. K. Williams, E. Gostick, D. A. Price, D. U. Soudamini, K. K. Voon, M. Olivo, J. Rossjohn, L. Mori, G. De Libero, Butyrophilin 3A1 binds phosphorylated antigens and stimulates human γδ T cells. *Nat Immunol* **14**, 908 916.
53. A. Sandstrom, C.-M. Peigné, A. Léger, J. E. Crooks, F. Konczak, M.-C. Gesnel, R. Breathnach, M. Bonneville, E. Scotet, E. J. Adams, The intracellular B30.2 domain of butyrophilin 3A1 binds phosphoantigens to mediate activation of human Vγ9Vδ2 T cells. *Immunity* **40**, 490 500.
54. M. R. Mamedov, S. Vedova, J. W. Freimer, A. Das Sahu, A. Ramesh, M. M. Arce, A. D. Meringa, M. Ota, P. A. Chen, K. Hanspers, V. Q. Nguyen, K. A. Takeshima, A. C. Rios, J. K. Pritchard, J. Kuball, Z. Sebestyen, E. J. Adams, A. Marson, CRISPR screens decode cancer cell pathways that trigger γδ T cell detection. | *Nature* | **621** (2023), doi:10.1038/s41586-023-06482-x.
55. J. Fisher, P. Abramowski, N. D. Wisidagamage Don, B. Flutter, A. Capsomidis, G. W.-K. Cheung, K. Gustafsson, J. Anderson, Avoidance of On-Target Off-Tumor Activation Using a Co-stimulation-Only Chimeric Antigen Receptor. *Molecular Therapy* **25** (2017), doi:10.1016/j.ymthe.2017.03.002.

56. S. Rafiq, O. O. Yeku, H. J. Jackson, T. J. Purdon, D. G. van Leeuwen, D. J. Drakes, M. Song, M. M. Miele, Z. Li, P. Wang, S. Yan, J. Xiang, X. Ma, V. E. Seshan, R. C. Hendrickson, C. Liu, R. J. Brentjens, Targeted delivery of a PD-1-blocking scFv by CAR-T cells enhances anti-tumor efficacy *in vivo*. *Nat Biotechnol* **36**, 847 856.
57. B. D. Choi, X. Yu, A. P. Castano, A. A. Bouffard, A. Schmidts, R. C. Larson, S. R. Bailey, A. C. Boroughs, M. J. Frigault, M. B. Leick, I. Scarfò, C. L. Cetrulo, S. Demehri, B. V Nahed, D. P. Cahill, H. Wakimoto, W. T. Curry, B. S. Carter, M. V Maus, CAR-T cells secreting BiTEs circumvent antigen escape without detectable toxicity. *Nat Biotechnol* **37**, 1049–1058 (2019).
58. E. R. Suarez, D. K. Chang, J. Sun, J. Sui, G. J. Freeman, S. Signoretti, Q. Zhu, W. A. Marasco, Chimeric antigen receptor T cells secreting anti-PD-L1 antibodies more effectively regress renal cell carcinoma in a humanized mouse model. *Oncotarget* **7**, 34341 34355.
59. J. S. Frieling, L. Tordesillas, X. E. Bustos, M. C. Ramello, R. T. Bishop, J. E. Cianne, S. A. Snedal, T. Li, C. H. Lo, J. de la Iglesia, E. Roselli, I. Benzaïd, X. Wang, Y. Kim, C. C. Lynch, D. Abate-Daga, γδ-Enriched CAR-T cell therapy for bone metastatic castrate-resistant prostate cancer. *Sci Adv* **9**, eadf0108 (2023).
60. A. H. Long, W. M. Haso, J. F. Shern, K. M. Wanhainen, M. Murgai, M. Ingaramo, J. P. Smith, A. J. Walker, M. E. Kohler, V. R. Venkateshwara, R. N. Kaplan, G. H. Patterson, T. J. Fry, R. J. Orentas, C. L. Mackall, 4-1BB costimulation ameliorates T cell exhaustion induced by tonic signaling of chimeric antigen receptors. *Nat Med* **21**, 581 590.
61. D. Gomes-Silva, M. Mukherjee, M. Srinivasan, G. Krenciute, O. Dakhova, Y. Zheng, J. M. S. Cabral, C. M. Rooney, J. S. Orange, M. K. Brenner, M. Mamonkin, Tonic 4-1BB Costimulation in Chimeric Antigen Receptors Impedes T Cell Survival and Is Vector-Dependent. *Cell Rep* **21**, 17 26.
62. S. J. Priceman, E. A. Gerdts, D. Tilakawardane, K. T. Kennewick, J. P. Murad, A. K. Park, B. Jeang, Y. Yamaguchi, X. Yang, R. Urak, L. Weng, W.-C. Chang, S. Wright, S. Pal, R. E. Reiter, A. M. Wu, C. E. Brown, S. J. Forman, Co-stimulatory signaling determines tumor antigen sensitivity and persistence of CAR T cells targeting PSCA+ metastatic prostate cancer. (2017), doi:10.1080/2162402X.2017.1380764.
63. T. Chen, J. Berenson, R. Vescio, R. Swift, A. Gilchick, S. Goodin, P. LoRusso, P. Ma, C. Ravera, F. Deckert, H. Schran, J. Seaman, A. Skerjanec, Pharmacokinetics and Pharmacodynamics of Zoledronic Acid in Cancer Patients with Bone Metastases. *The Journal of Clinical Pharmacology* **42**, 1228–1236 (2002).
64. Z. Sebestyen, I. Prinz, J. Déchanet-Merville, B. Silva-Santos, J. Kuball, Translating gammadelta (γδ) T cells and their receptors into cancer cell therapies. , doi:10.1038/s41573-019-0038-z.
65. C. Harmon, A. Zaborowski, H. Moore, P. St Louis, K. Slattery, D. Duquette, J. Scanlan, H. Kane, B. Kunkemoeller, C. L. McIntyre, A. Ni Scannail, B. Moran, A. C. Anderson, D. Winter, D. Brennan, M. A. Brehm, L. Lynch, γδ T cell dichotomy with opposing cytotoxic and wound healing functions in human solid tumors. *Nature Cancer* | **4**, 1122–1137 (2023).

66. R. Finck, E. F. Simonds, A. Jager, S. Krishnaswamy, K. Sachs, W. Fantl, D. Pe'er, G. P. Nolan, S. C. Bendall, Normalization of mass cytometry data with bead standards, *Cytometry Part A* **83**, 483–494 (2013).

67. S. C. Bendall, E. F. Simonds, P. Qiu, E.-A. D. Amir, P. O. Krutzik, R. Finck, R. V. Bruggner, R. Melamed, A. Trejo, O. I. Ornatsky, R. S. Balderas, S. K. Plevritis, K. Sachs, D. Pe'er, S. D. Tanner, G. P. Nolan, Single-cell mass cytometry of differential immune and drug responses across a human hematopoietic continuum, *Science* **332**, 687–696 (2011).

68. He A, Huang Y, Cheng W, Zhang D, He W, Bai Y, Gu C, Ma Z, He Z, Si G, Chen B, Breault D, Dong M, Xiang D, Organoid culture system for patient-derived lung metastatic osteosarcoma. *Medical Oncology* **37(**11) 105 (2020*)*

Acknowledgments

The authors would like to thank Ayad Eddaoudi from the UCL-Great Ormond Street Institute of Child Health Flow Cytometry Core Facility and Yanping Guo from the UCL Cancer Institute Cytometry Core Facility for their assistance with data collection. Osteosarcoma patient-derived xenograft lines were supplied by KS and MCM under an MTA. This work is supported by the NIHR GOSH BRC.

Funding

This work was supported by the UKRI Medical Research Council (MR/T028270/1 CT), Cancer Research UK (C60693/A23783 to CT), the Cancer Research UK City of London Centre (C7893/A26233 to CT), the UCLH Biomedical Research Centre (BRC422 to PV), the Cancer Research UK City of London Centre Clinical Academic Training Program Award (C355/A28852 to JF, CT, and CN), the Academy of Medical Sciences (SGL024/1022 to JF), the NIHR (CL-2019-18-007 to JF), the UCL Tech Fund (UTF-20-006/Fisher/UCL to JF, MB, and JA), the GOSH Charity (VS0119 to JF), and The Wellcome Trust (214046/Z/18/Z to JF). This work was also supported by a Stand up to Cancer/CRUK Pediatric Cancer New Discoveries Challenge stage 2 award (RT6188, to JA), Action Medical Research/LifeArc (GN2927, to JA and MB), and the Research in Childhood Cancer discretionary fund (to JA). Support for the establishment of PDX and PDX-derived cell lines came from the European Union (ERANET TRANSCAN-2_TORPEDO ER-2015–2360405 to KS) and from Fondazione AIRC under IG2019-ID. 22805 project (to KS).

Author contributions

DF wrote the manuscript, devised, and performed in vitro experiments pertaining to expansion and function of γδ T cells, analyzed and compiled the overall dataset. MB edited the manuscript, provided supervision during the project and contributed to the conceptualization of the work. AS performed the experiments on γδ T cell armoring with IL-15 derived constructs and assisted DF in the experimental setup. CN produced and analyzed the suspension-cell CyTOF data. EH performed experiments using OPS-γδ and some of comparisons of OPS-γδ and CAR-γδ T cells. EV performed in vivo experiments with osteosarcoma. AK manufactured lentivirus for the project and supported the work by providing maintenance of cell cultures. JC provided the lentiviral backbones and envelopes used in this study. ER provided know-how regarding binder design and characterized the SM3EL binder. PV performed the 3D osteosarcoma/γδ T cell co-cultures and collected CyTOF data from these experiments. BD performed in vivo experiments using subcutaneous SUP-T1. TDM and AF performed in vitro experiments on γδ T cell function and cytotoxicity. HB performed the Western Blotting experiments to characterize secreted products. ATB performed in vitro experiments pertaining to γδ T cell function and manufactured engineered γδ T cells at scale for in vivo experiments. KS and MCM supervised the creation of osteosarcoma patient-derived xenograft lines. CT secured funding to support the mass cytometric elements of this study and supervised the work of CN, together with JF. KC provided knowledge and guidance regarding antibody biology. JA contributed to the editing of the manuscript and to the devising of experiments. JF conceived the idea, secured the funding, performed in vitro experiments and analyzed in vitro and in vivo datasets in this work.

Competing Interests

JA declares founder shares in Autolus Ltd and collaborations with Roche and ALX-Oncology. JF, JA, ER and KC are inventors of a patent pertaining to opsonin-secreting immune cells (WO2021148788A1). JF, DF, JC and MB are inventors of a patent pertaining to methods of engineering innate lymphocytes (WO2023180759A1). JA, KC and MB are inventors of a patent pertinent to cellular immunotherapy development (WO2024009075A1). MB has carried out advisory work for LAVA Therapeutics. BD holds equity in cell therapy companies Leucid Bio and Autolus.

KC has no other conflicting interests to declare. AS, CN, EV, AK, PV, BD, TDM, AF, HB, KS and MCM have no conflicts of interest to declare.

Data availability

All data associated with this study are in the paper or supplementary materials. Tabulated forms of all datasets shown in this manuscript are available at https://doi.org/10.5061/dryad.q2bvq83t1. Code generated as part of this study are available at https://zenodo.org/doi/10.5281/zenodo.10993244.

1106
1107